Primary and secondary radiation detection for range verification through Prompt Gamma Timing technique

S Giordanengo – INFN Torino

E. M. Data[1], F. M. Milian[1,3], S. Ranjbar[1,2], P. Cerello[1], R. Cirio[1,2], M. Donetti[4], V. Ferrero[1,2], M. A. Fadavi Mazinani[1], D. M. Montalvan Olivares[1,2], F. Pennazio[1], M. Pullia[4], I. B. Rivas Ortiz[1], R. Sacchi[1,2], A. Vignati[1,2], E. Fiorina[1]

1. Istituto Nazionale di Fisica Nucleare (INFN)– Sezione di Torino

2. Università di Torino, Torino

3. State University of Santa Cruz, Ilhéus, BA, Brazil

4. Centro Nazionale di Adroterapia Oncologica, Pavia

INFN

UNIVERSITÀ DI TORINO

CNAO
Centro Nazionale di Adroterapia Oncologica

FONDAZIONE BRUNO KESSLER

Outline

- Prompt gamma for in-vivo Range Verification
- Prompt Gamma Timing method
- Experimental setup
- Preliminary results with carbon ions
- Future perspectives

Range uncertainties in particle therapy

Clinical motivation for in-vivo range verification system: morphological changes

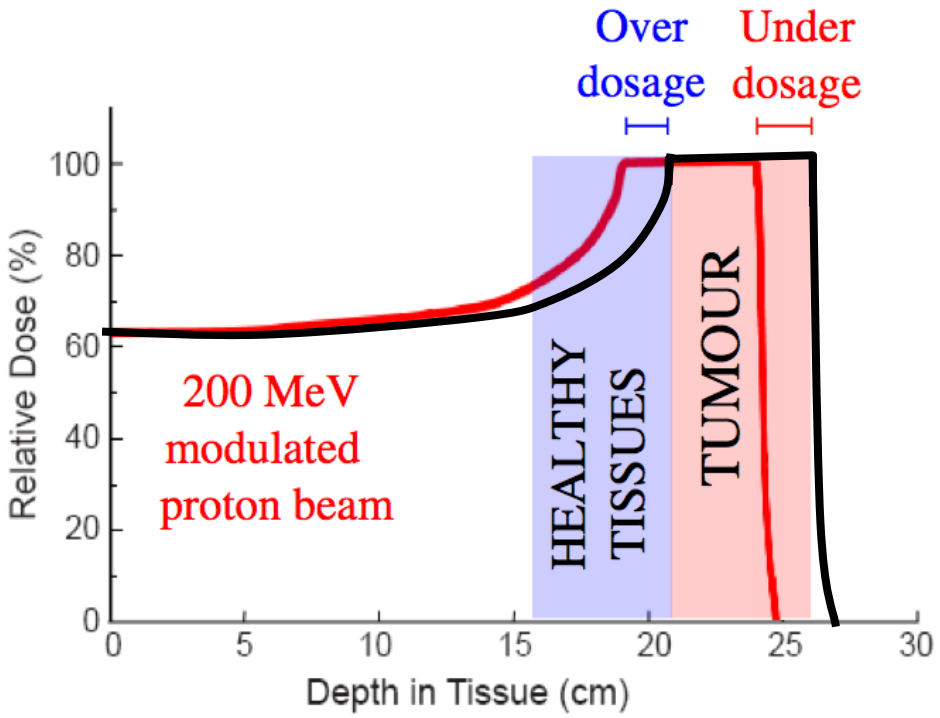

Zhu X, Fakhri GE. *Theranostics. 2013;3(10):731-740.*

Planning CT

Control CT

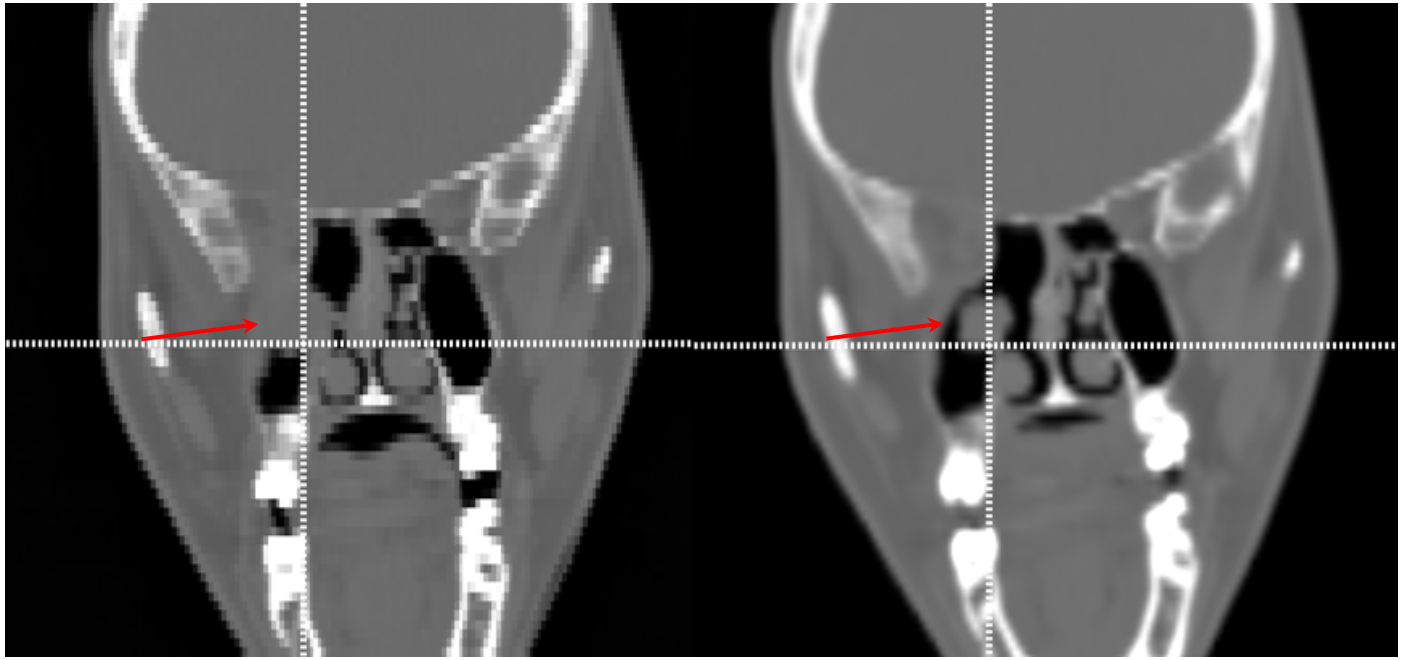

Air cavities induce large range variations

Range uncertainties in particle therapy

Clinical motivation for in-vivo range verification system: morphological changes

MC simulations using two CT scans of the same patient taken at different times.

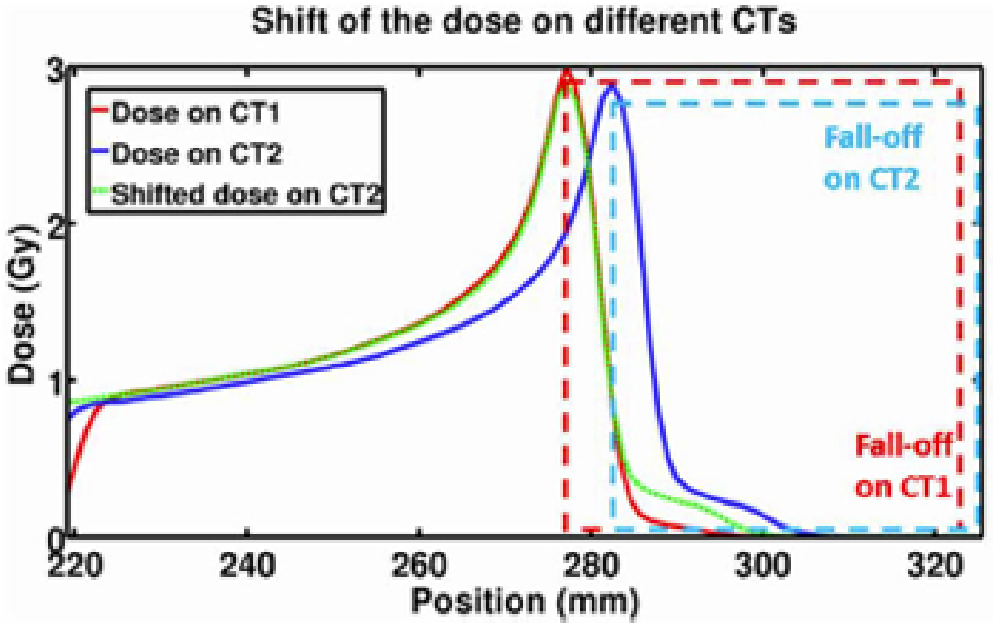

Ref. M. Pinto - Eur. Phys. J. Plus (2024) 139:884
10.1140/epjp/s13360-024-05664-4

Planning CT

Control CT

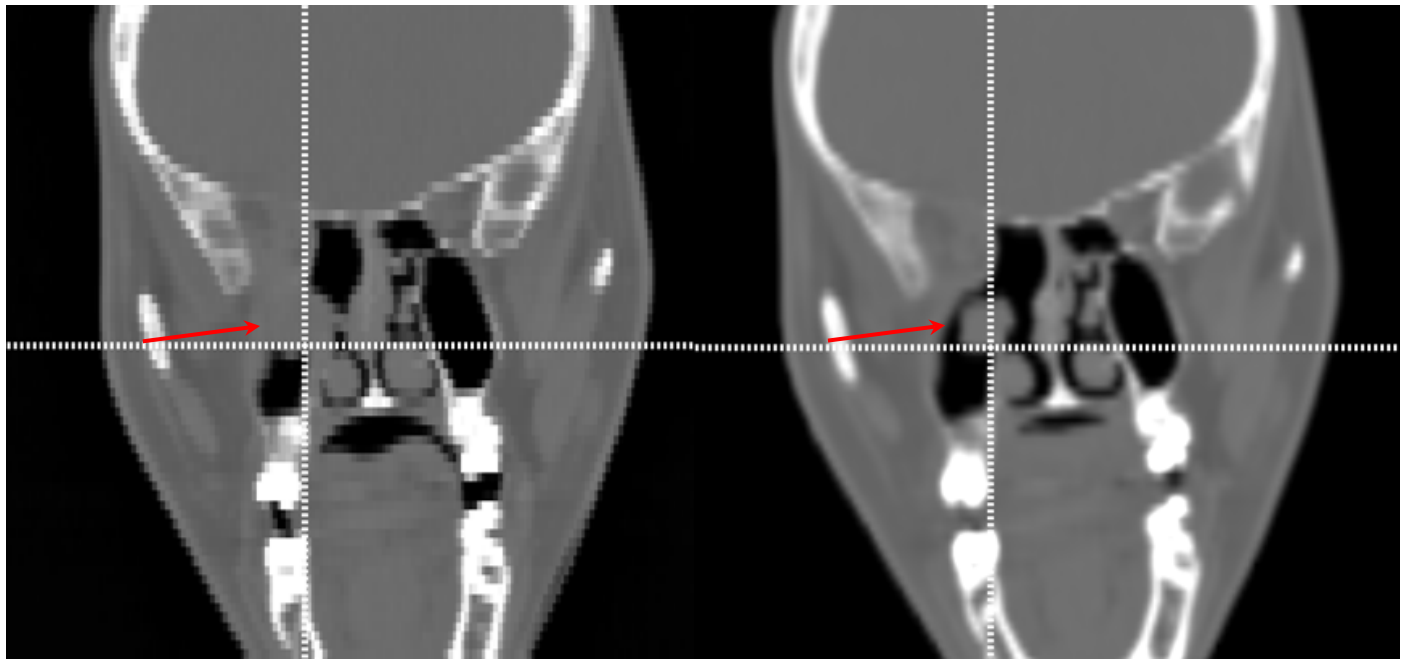

Treatment optimization thanks to margin reduction

In-vivo range verification techniques exploit secondary radiations

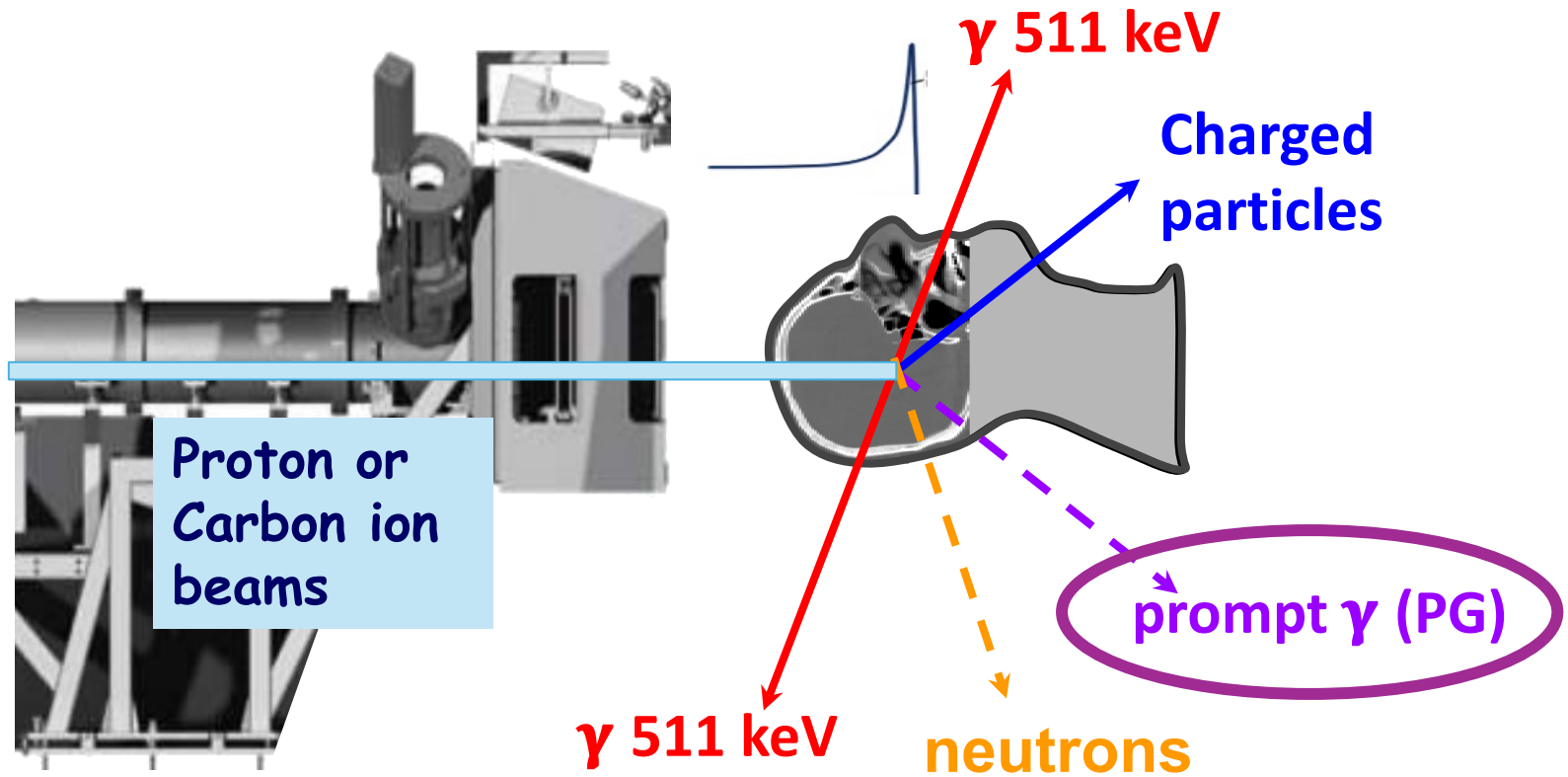

Courtesy of Ferrero, Pennazio, Fiorina

Prompt Gamma Emission

Prompt–gamma imaging in particle therapy

Review | Open access | Published: 09 October 2024
Volume 139, article number 884, (2024) Cite this article

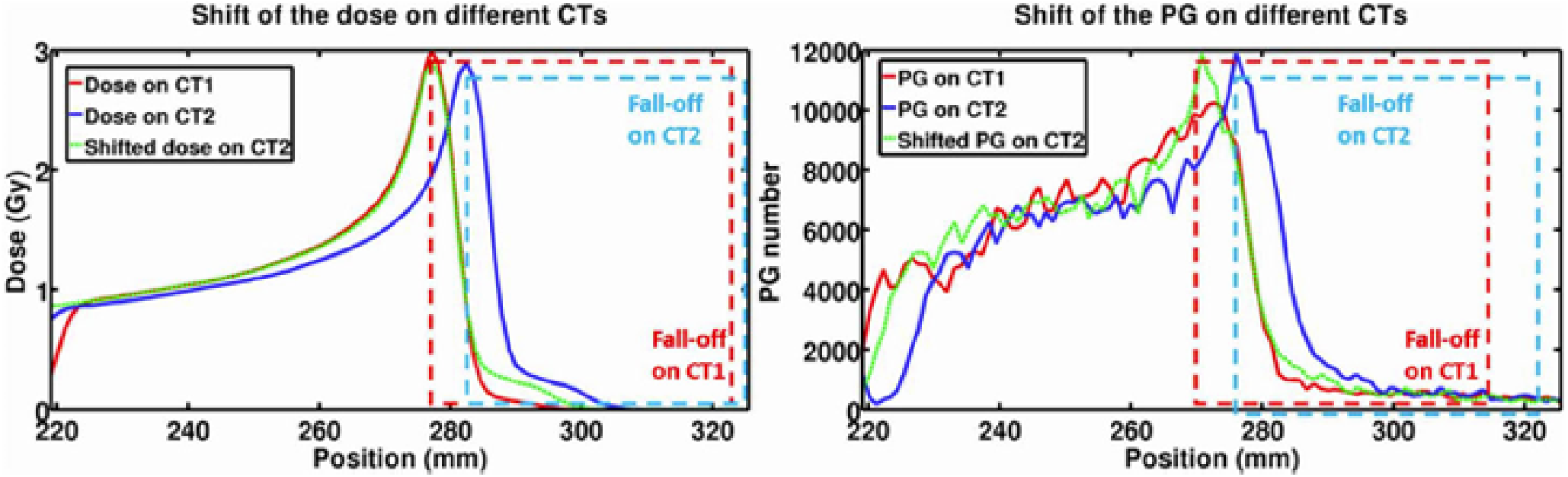

MC simulations using two CT scans of the same patient taken at different times. Dose (left) and PG (right) distributions of the same pencil beam on the two CT scans are shown.

Prompt Gamma Energy

The broad PG energy spectrum

Measured PG energy spectra for 226.7 MeV (black) and 162.0 MeV (blue) proton beam energies in a PMMA phantom

T. Werner et al. Phys. Med. Biol. 64 **(2019)** 105023

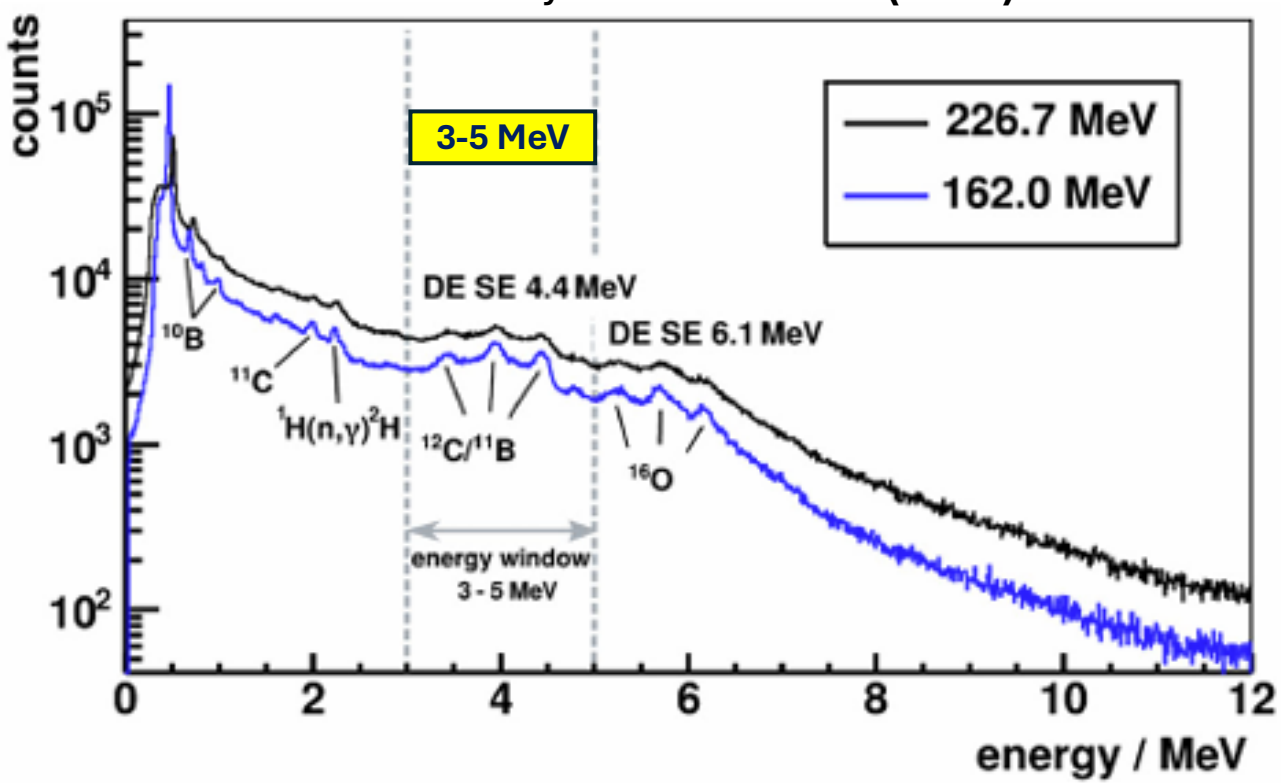

The ground state transition in ^{16}O, ^{11}B and ^{12}C are pointed out, including their respective single (SE) and double escape peaks (DE). PG ray transitions from ^{10}B, ^{11}C and $^{1}H(n,\gamma)^{2}H$ are also visible in the low energy part. The spectra shown had no background subtraction procedure.

Prompt gamma energy spectra from ions

PIBS: Proton and ion beam spectroscopy for *in vivo* measurements of oxygen, carbon, and calcium concentrations in the human body

Paulo Magalhaes Martins, Riccardo Dal Bello, Benjamin Ackermann, Stephan Brons, German Herma
Thomas Kihm & Joao Seco

Scientific Reports **10**, Article number: 7007 (2020) | Cite this article

2020

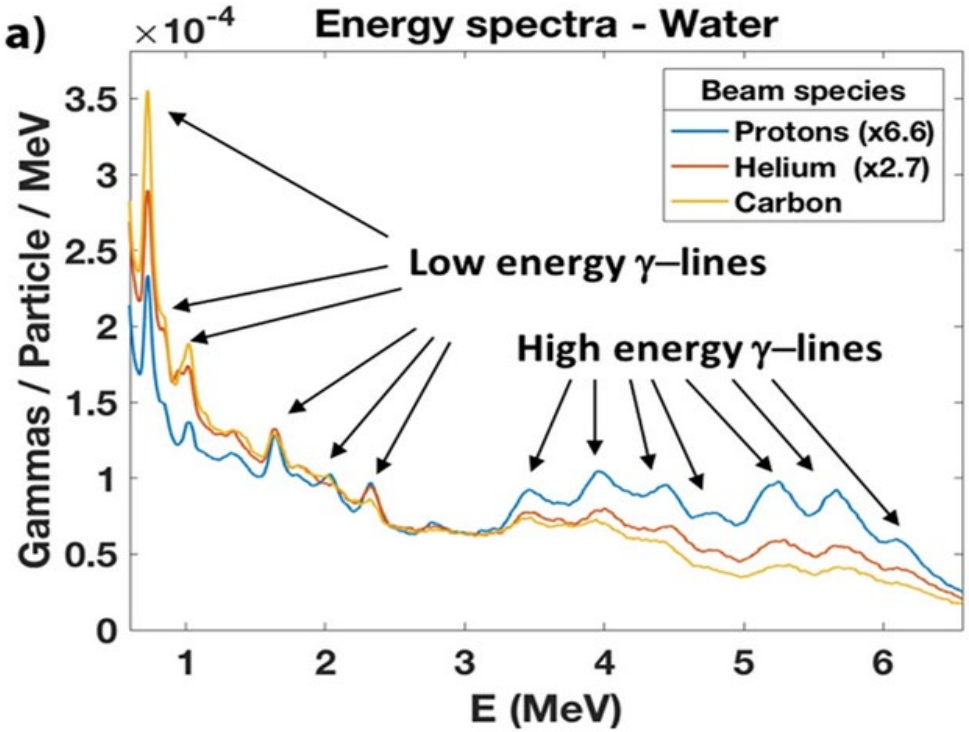

Energy spectra obtained from the irradiation of water by protons, helium, and carbon beams. (**a**) The low energy -lines, particularly the 0.718-MeV carbon line, show a higher prominence for carbon beams, while the high energy -lines show a higher prominence for proton and helium beams.

Total Prompt Gamma Emission

Simulated total gamma emission during irradiation of tissue. For reference, the energy deposited by thep rotons (Bragg curve) is also shown.

Simulation of prompt gamma-ray emission during proton radiotherapy

2012

Joost M Verburg[1,2], **Helen A Shih**[1] **and Joao Seco**[1]

[1] Department of Radiation Oncology, Harvard Medical School and Massachusetts General Hospital, Boston, MA 02114, USA
[2] School of Medical Physics and Engineering, Eindhoven University of Technology, Eindhoven, The Netherlands

E-mail: jverburg@fas.harvard.edu

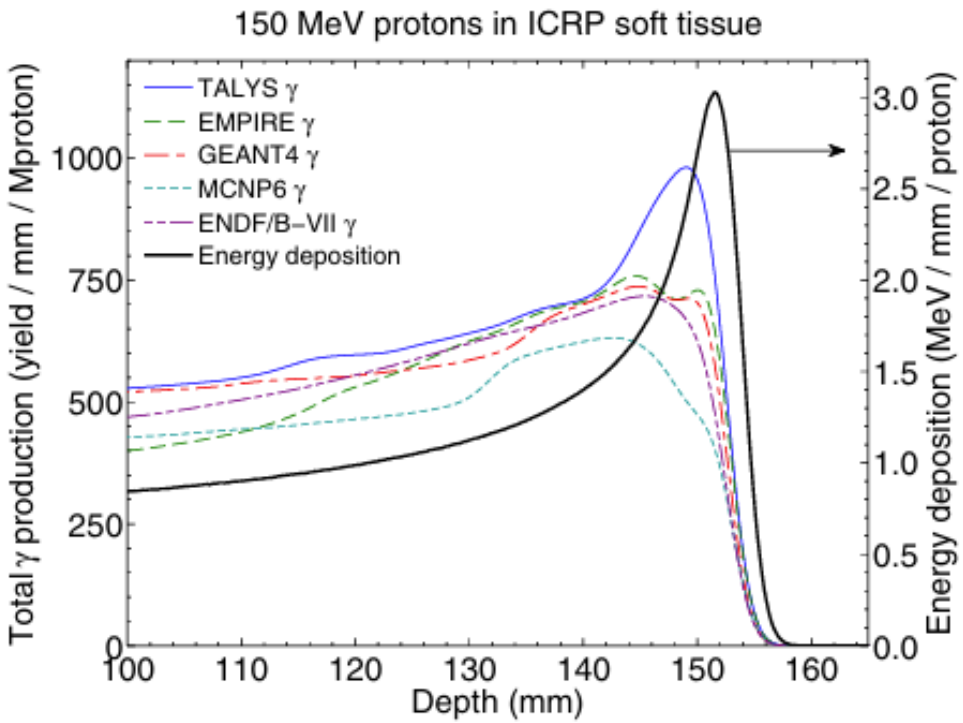

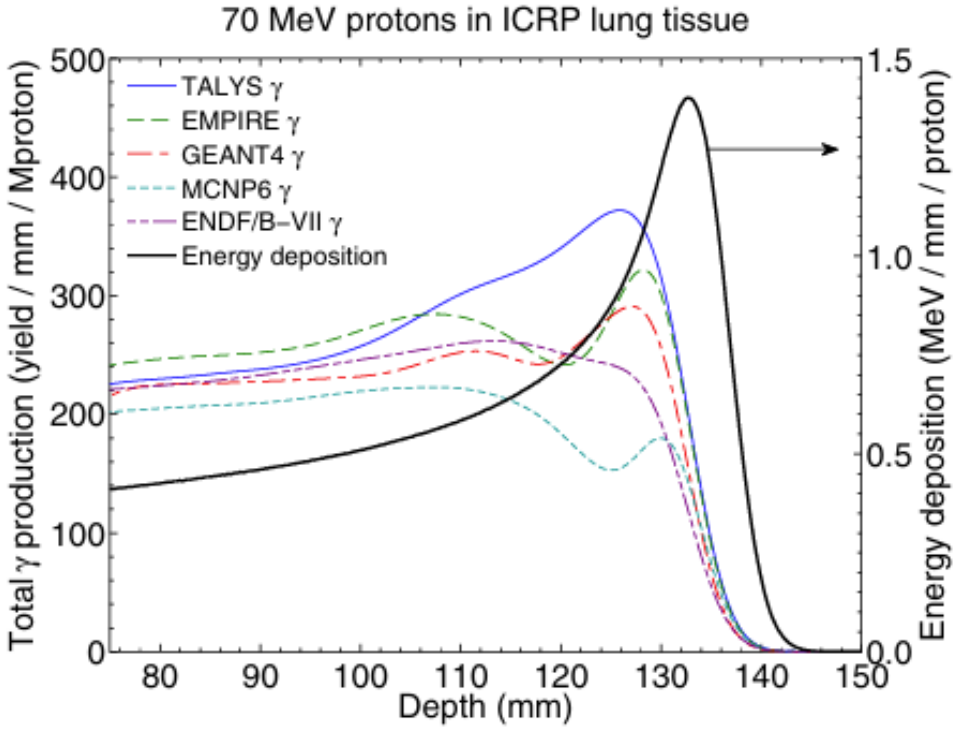

Prompt Gamma Emission

Simulated 4.44 and 6.13 MeV gamma emission during irradiation of ICRP soft tissue with 150 MeV protons. Bragg curve is also shown.

Simulation of prompt gamma-ray emission during proton radiotherapy

2012 Verburg[1,2], Helen A Shih[1] and Joao Seco[1]

[1] Department of Radiation Oncology, Harvard Medical School and Massachusetts General Hospital, Boston, MA 02114, USA
[2] School of Medical Physics and Engineering, Eindhoven University of Technology, Eindhoven, The Netherlands

E-mail: jverburg@fas.harvard.edu

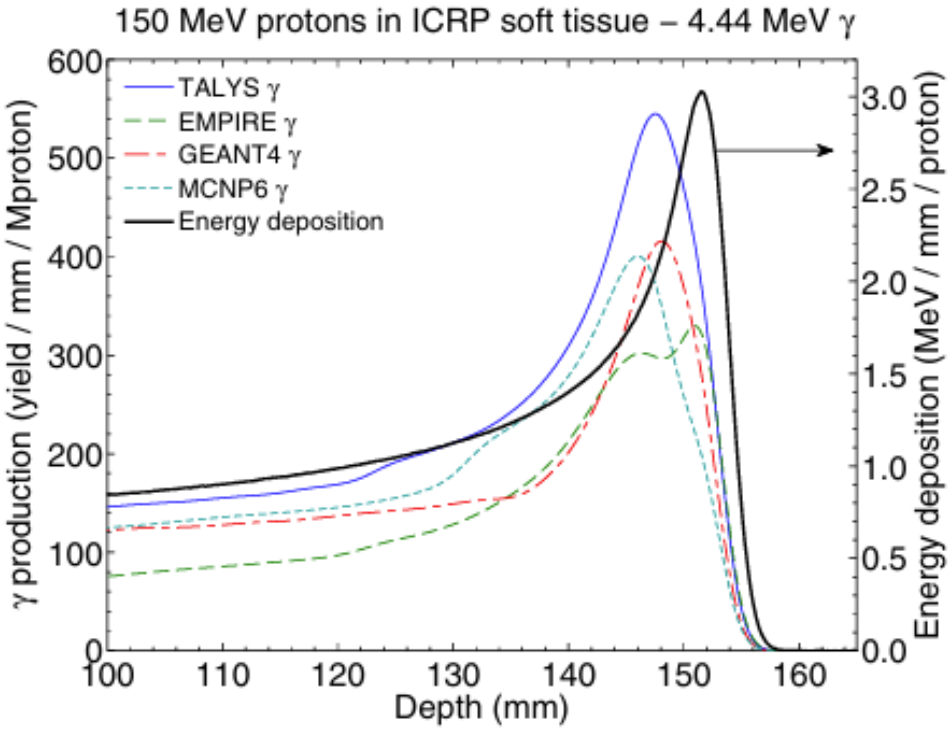

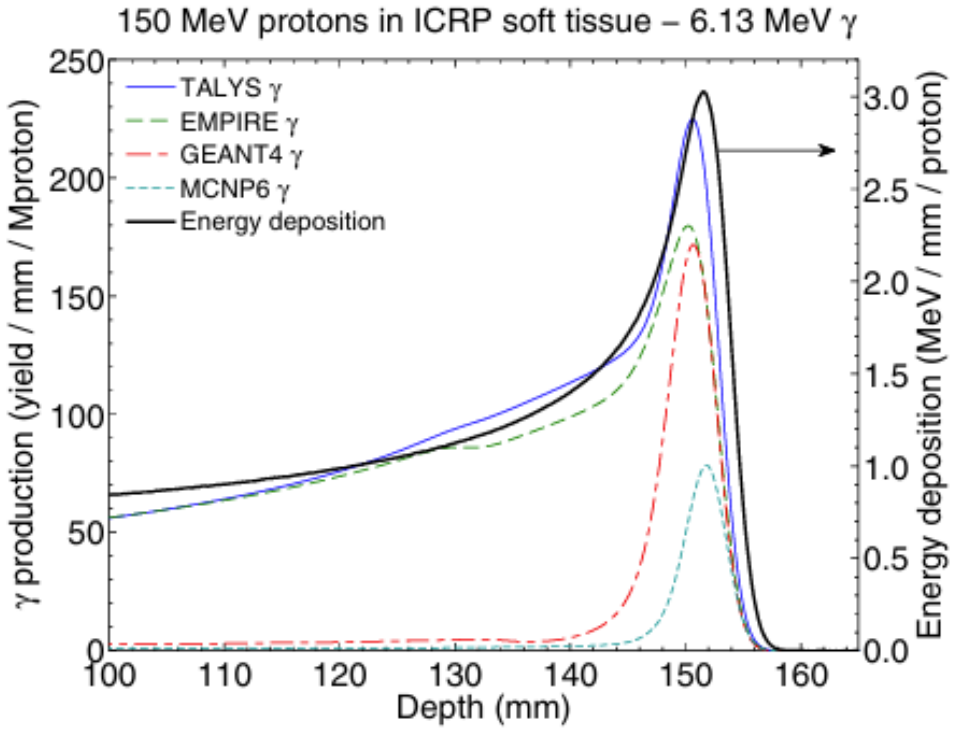

In-vivo treatment monitoring with prompt γ

Techniques to detect prompt γ (E ~ 2-8 MeV)

- Collimated gamma camera →PG Imaging
- Compton Camera → PG Imaging
- Prompt gamma Timing → PG Range verification

Prompt–gamma imaging in particle therapy

Review | Open access | Published: 09 October 2024

Volume 139, article number 884, (2024) Cite this article

Ref. M. Pinto - Eur. Phys. J. Plus (2024) 139:884
10.1140/epjp/s13360-024-05664-4

2024

Prompt gamma imaging system in particle therapy: a mini-review

Bo-Wi Cheon Chul Hee Min*

MINI REVIEW article
Front. Phys., 13 May 2024
Sec. Medical Physics and Imaging
Volume 12 - 2024
| https://doi.org/10.3389/fphy.2024.1356572

In-vivo proton treatment monitoring with prompt γ

Techniques to detect prompt γ E ~ 2-8 MeV

- Collimated gamma camera → PG Imaging

The first usage of the knife-edge slit camera in a patient was reported in 2016 from the proton therapy centre at the Universitäts Protonen Therapie Dresden (UPTD) at OncoRay (Dresden, Germany),
- passive scattered proton therapy treatment
- the PG camera monitoring the treatment

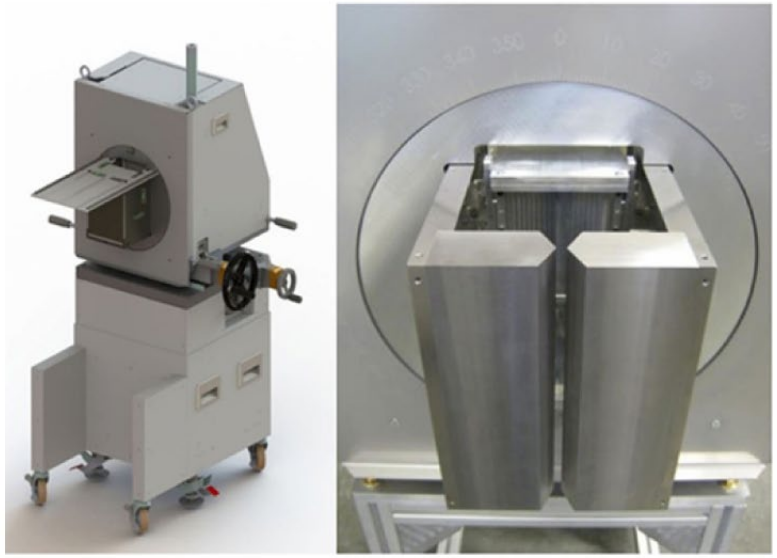

Fig. 5 Knife-edge slit camera prototype. The complete trolley positioning system is drawn on the left, and a photo of the knife-edge slit collimator is shown on the right. Reproduced from [150] under the terms of the Creative Commons Attribution License (CC BY, https://creativecommons.org/licenses/by/4.0/)

C. Richter et. al, *First clinical application of a prompt gamma based in vivo proton range verification system*. Radiother. Oncol. 118(2), 232–237 (2016). 10.1016/j.radonc.2016.01.004

scientific reports

https://doi.org/10.1038/s41598-024-72870-6

2024

Check for updates

OPEN

First experimental verification of prompt gamma imaging with carbon ion irradiation

Aicha Bourkadi Idrissi[1,2]✉, Giacomo Borghi[1,2], Anita Caracciolo[1,2], Christian Riboldi[1,2], Marco Carminati[1,2], Marco Donetti[3], Marco Pullia[3], Simone Savazzi[3], Franco Camera[2,4] & Carlo Fiorini[1,2]✉

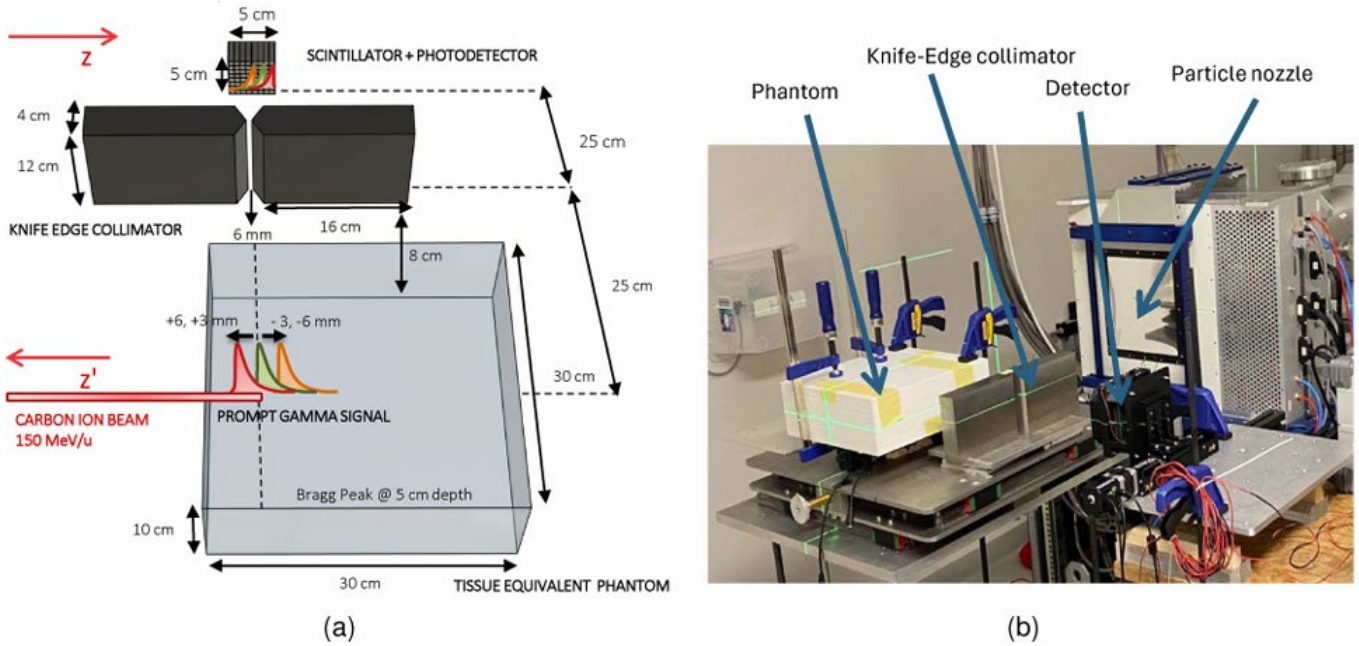

Fig. 3. (**a**) Knife Edge Slit Camera setup configuration at CNAO; the phantom and collimator axes, as well as the collimator axis and detector face, are separated by 25 cm. (**b**) Photo of the measurements setup at CNAO.

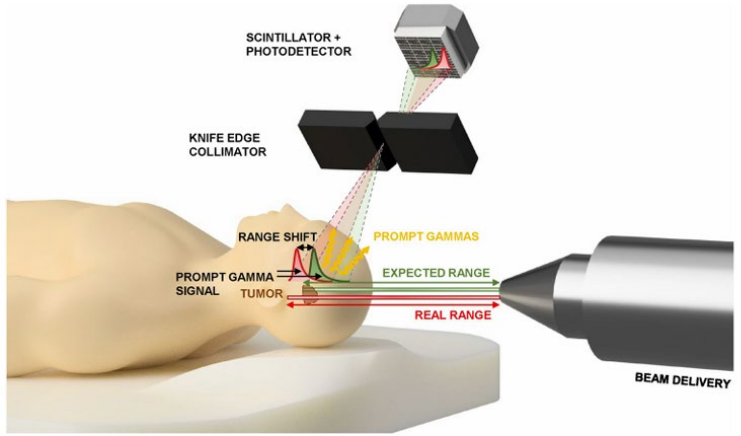

Fig. 1. Knife-edge slit camera concept of operation: deviations between real range and expected one are detected through PG signal projected to a pixellated camera thanks to a knife-edge slit collimator.

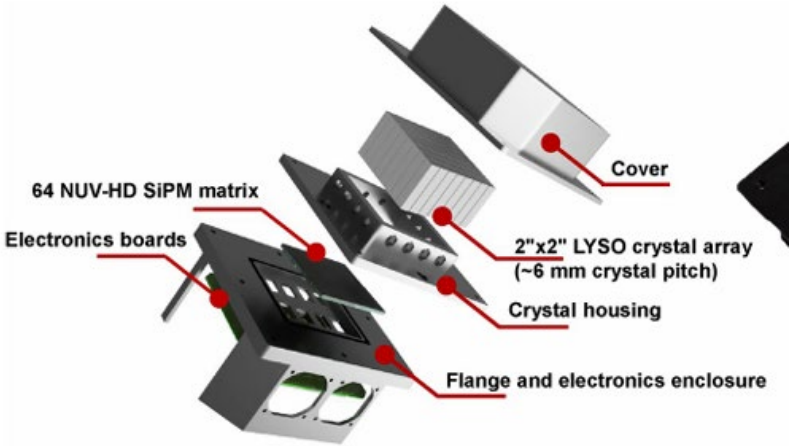

64-channel detector prototype for the experimental validation of PGI technique

In-vivo treatment monitoring with prompt γ

Techniques to detect prompt γ E ~ 2-8 MeV

- **Compton Camera → Prompt Gamma Imaging**

→ use the Compton scattering process
→ Perform electronic collimation

They comprise a scatterer and an absorber detector in the most straightforward design possible. Ideally, the incident photon scatters in the scatterer and is then fully absorbed in the absorber.

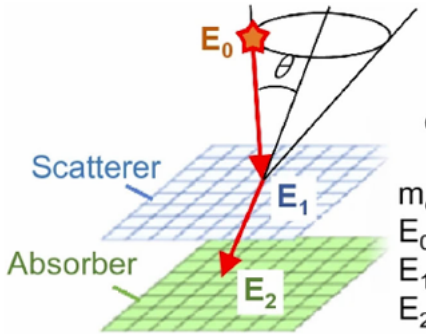

$$\cos\theta = 1 - m_e c^2 \left(\frac{1}{E_0 - E_1} - \frac{1}{E_0}\right)$$

$m_e c^2$: Electron rest energy
E_0 : Initial energy of the incident γ-ray
E_1 : Energy detected by the scatterer
E_2 : Energy detected by the absorber

M.Sakai et. al, Experimental study on Compton camera for boron neutron capture therapy applications. Sci. Rep. 13(1), 22883 (2023). https://doi.org/10.1038/s41598-023-49955-9

In-vivo treatment monitoring with prompt γ

Techniques to detect prompt γ E ~ 2-8 MeV

- Collimated gamma camera → PG Imaging
- Compton Camera → PG Imaging

- **Prompt gamma Timing**

Prompt Gamma Timing

Primaries:
- carbon ions
- Protons

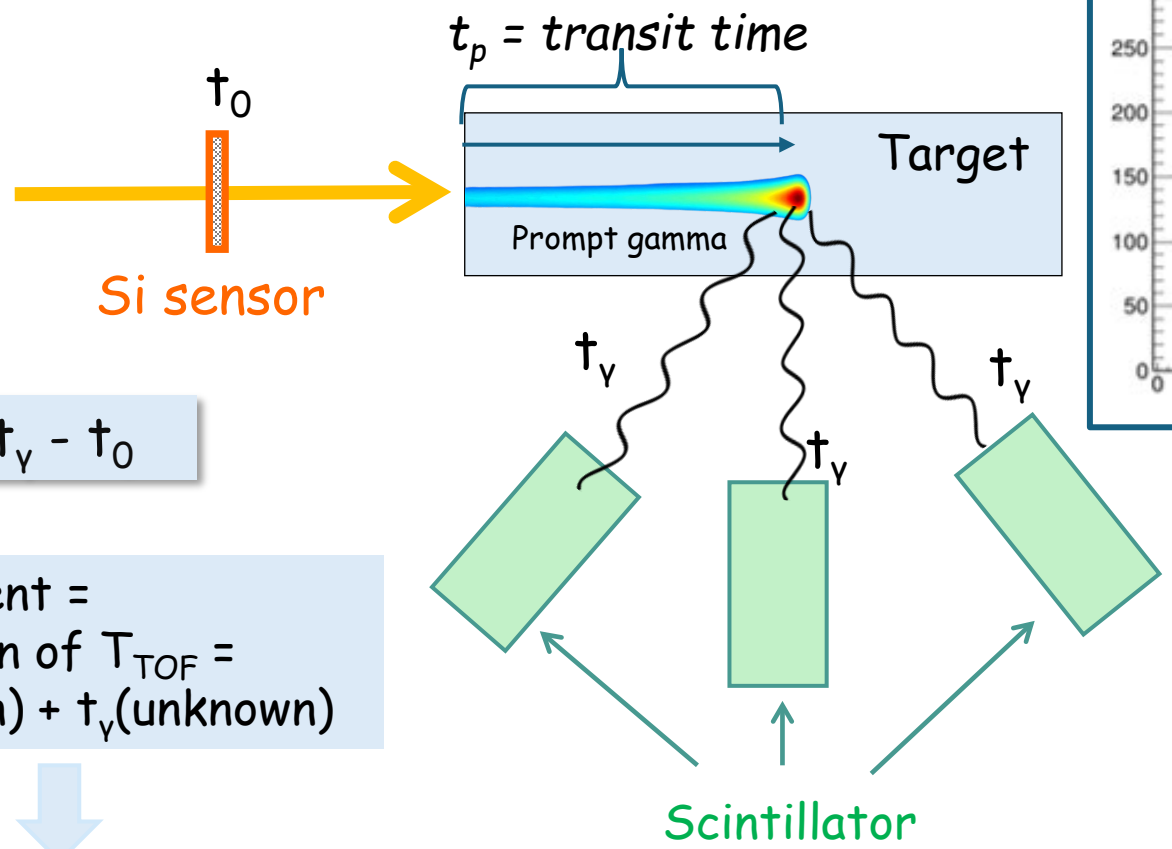

$ToF = t_\gamma - t_0$

Measurement =
Distribution of T_{TOF} =
t_p (unknown) + t_γ(unknown)

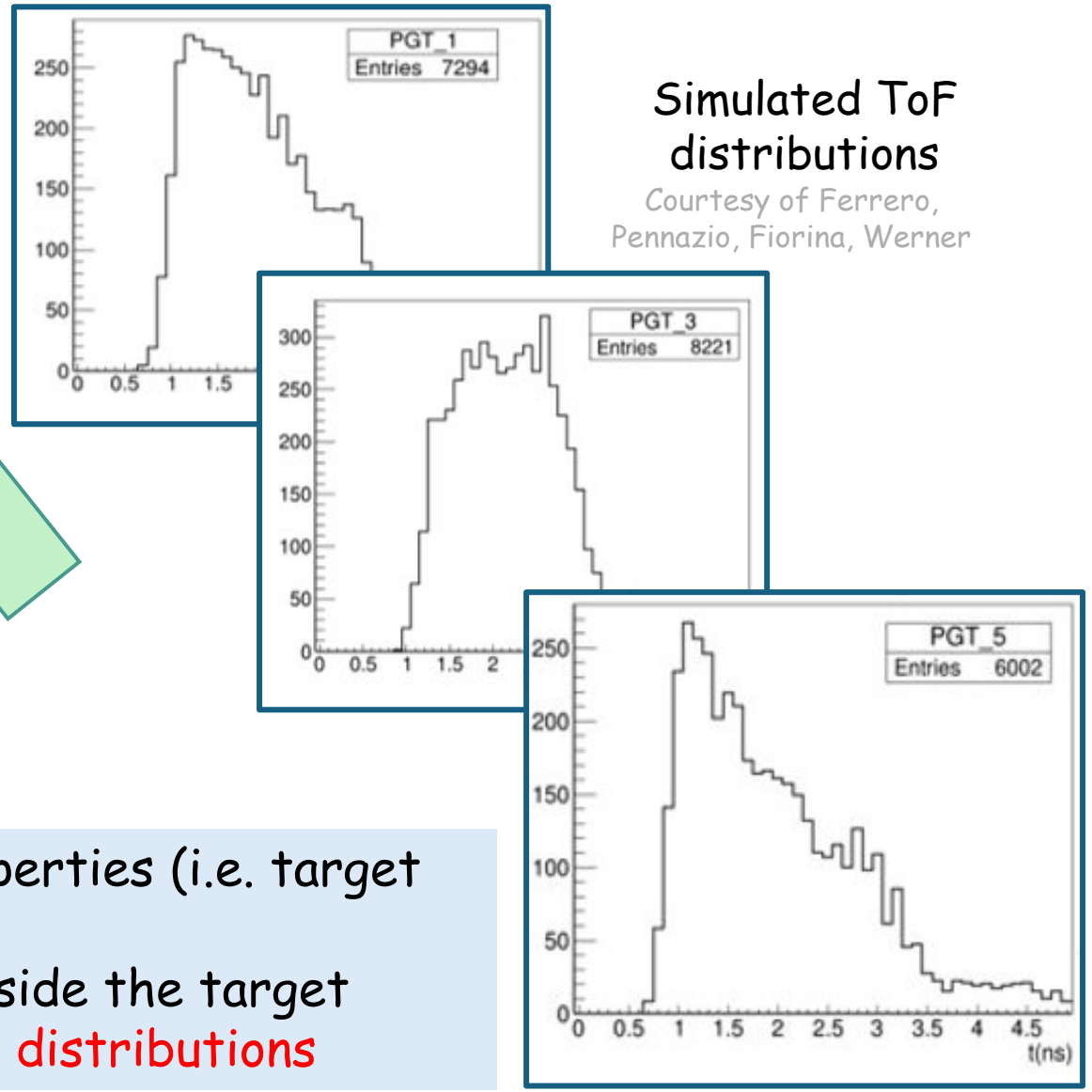

Simulated ToF distributions

Courtesy of Ferrero, Pennazio, Fiorina, Werner

Depend on initial beam energy (known) and target properties (i.e. target stopping power, unknown)

➔ its properties are related to the particle motion inside the target

➔ Range variations result in a different shape of ToF distributions

Setup for PGT measurements

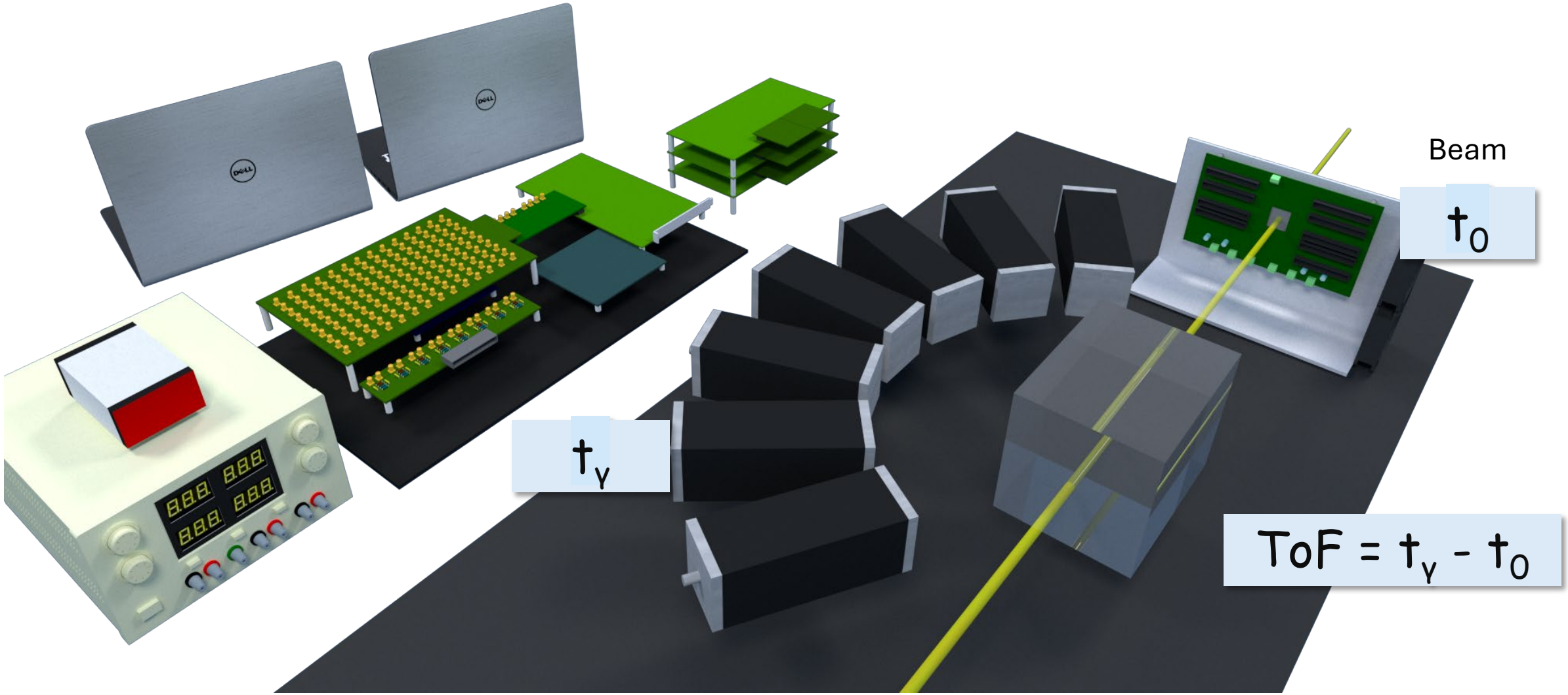

Setup for PGT measurements

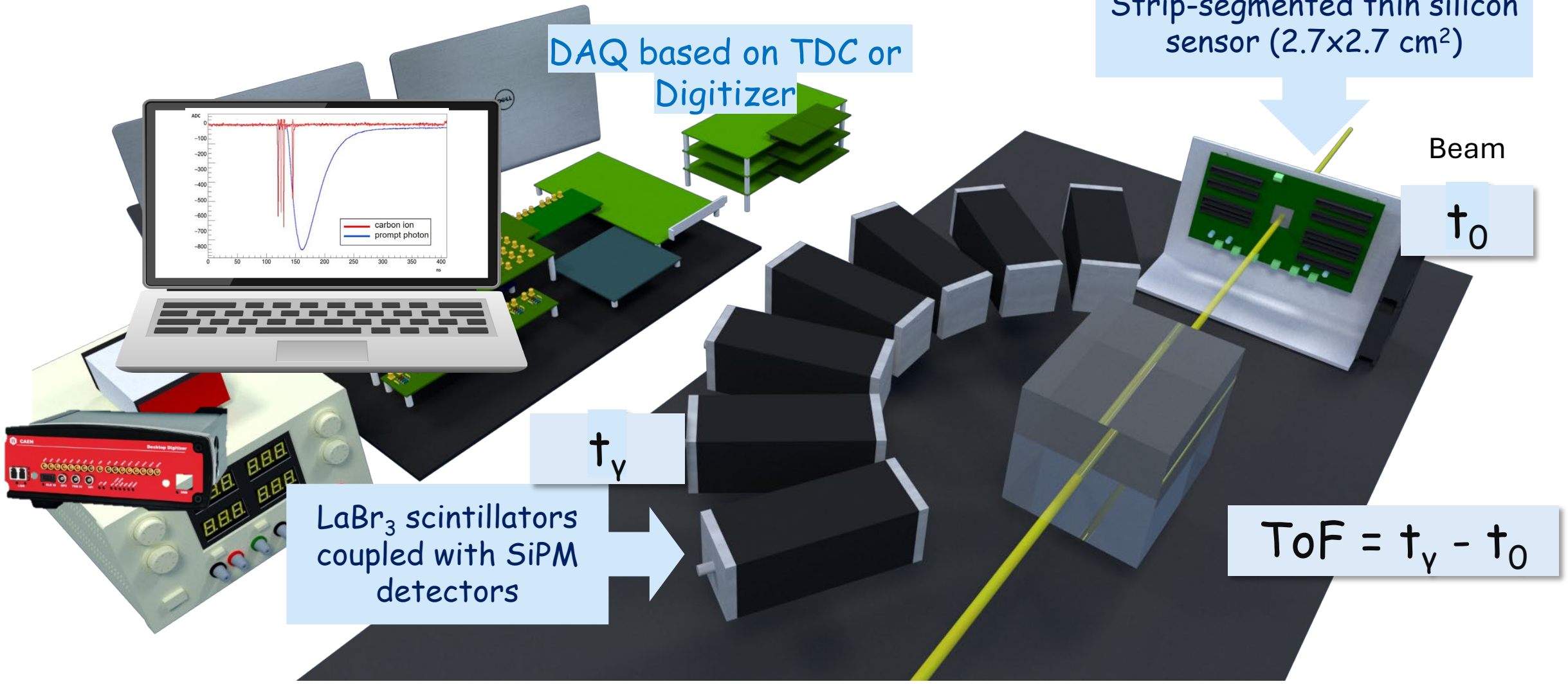

Detectors for primary beams

- 11-strips Si n-on-p sensor (FBK)
- 45-60 μm active thickness
- Total area of 17.6 mm²
- Short signal duration (< 2 ns)

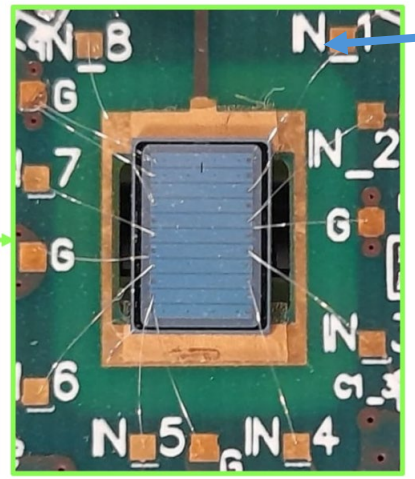

(b)

For protons we developed
Low Gain Avalanche Diode (LGAD) sensors
Thin p^+ gain layer implanted under the n^{++} cathode

- Controlled low gain (~ 10-30)
- Gain increases with bias voltage
- High Signal/Noise ratio

Each strip 2.2 mm² active area (3993 μm x 550 μm)

For protons: 8 strips with gain

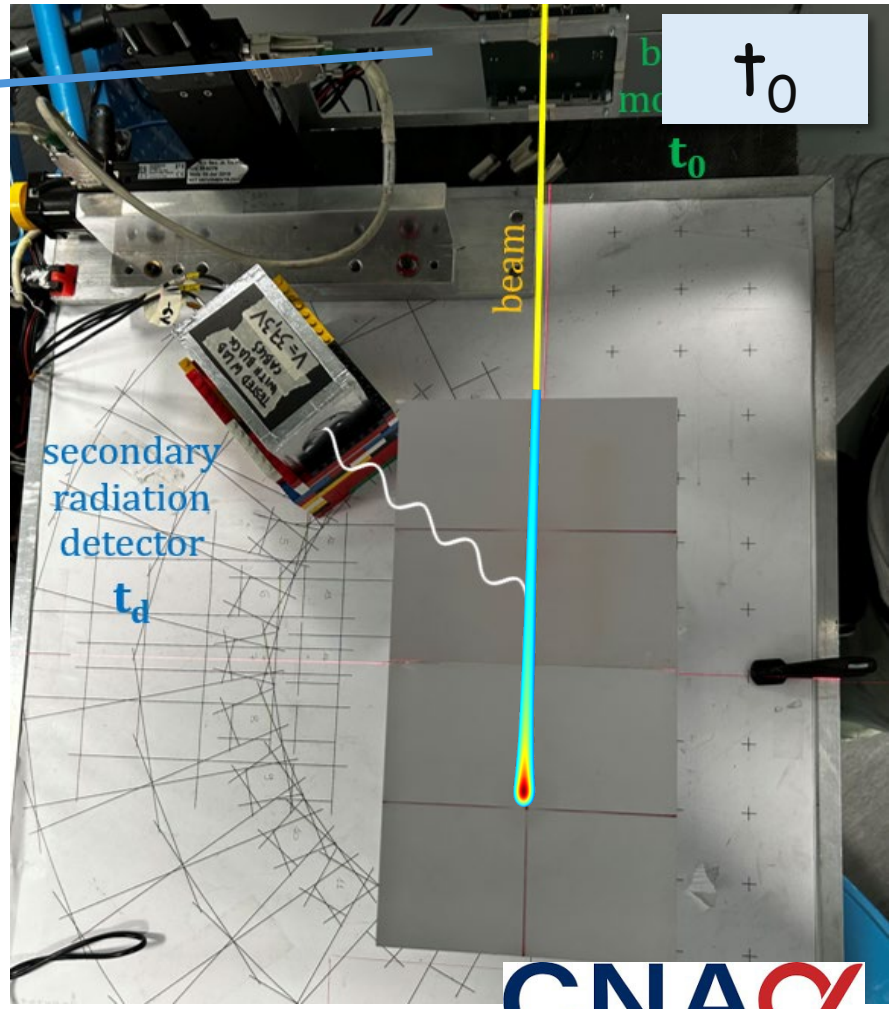

Detectors for primary beams

- 11-strips Si n-on-p sensor (FBK)
- 45-60 μm active thickness
- Total area of 17.6 mm²
- Short signal duration (< 2 ns)

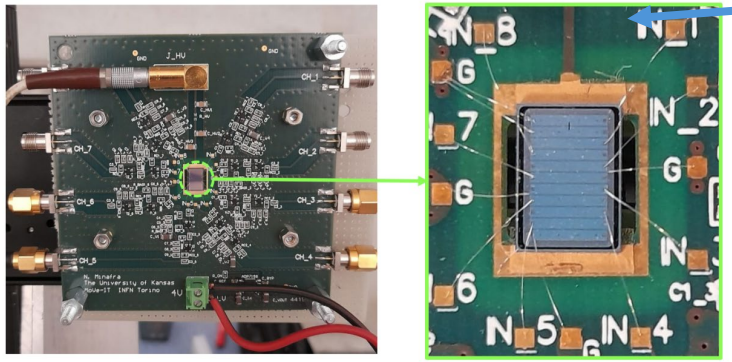

8 strips
with gain

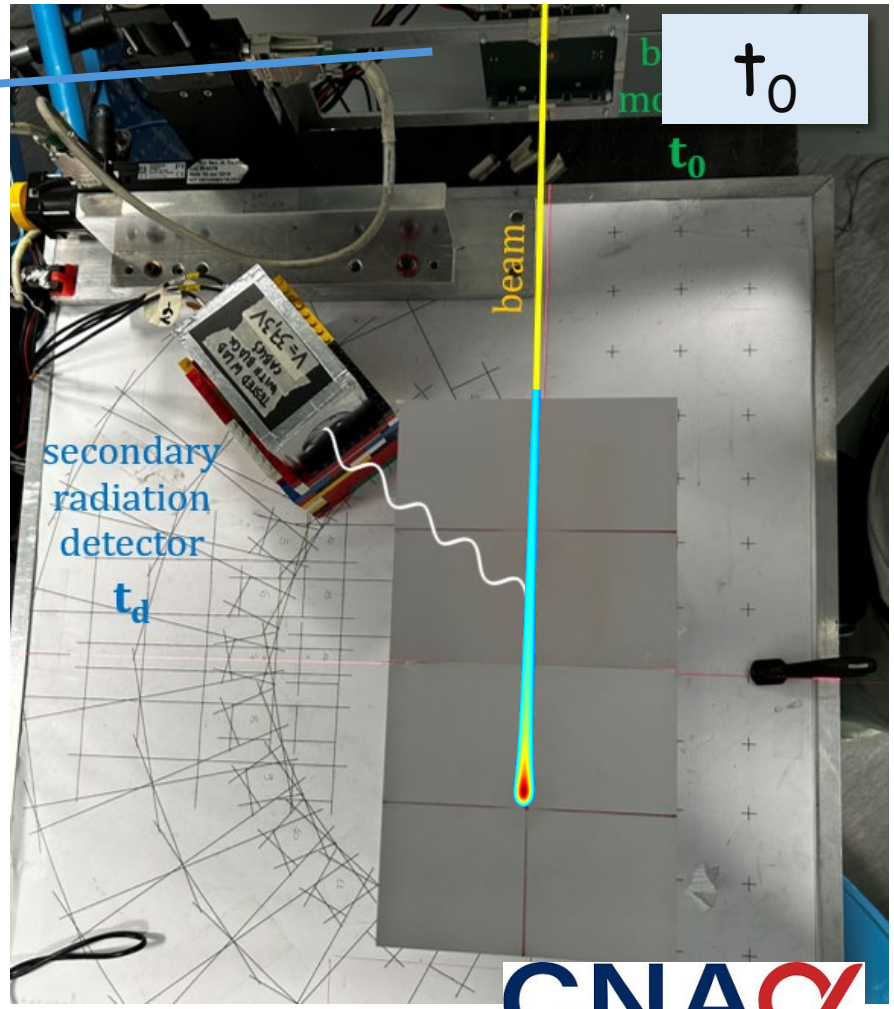

Frontend readout:
- 8-channels amplifier board

Time resolution single crossing
~ 30-75 ps (Carbon ion - protons)

Thin segmented silicon detectors for single ion tracking in carbon ion beam therapy: Performance insights

D.M. Montalvan Olivares [a,b] · F. Mas Milian [b,c] · O.A. Marti Villarreal [d] · ... · V. Sola [a,b] · A. Vignati [a,b] · S. Giordanengo [b] ... Show more

Volume 136, 105048, August 2025 · *Open Access*

DOI: 10.1016/j.ejmp.2025.105048 External Link

Single proton signals

Phys. Med. Biol. **68** (2023) 235009

Physics in Medicine & Biology 2023

Performance of LGAD strip detectors for particle counting of therapeutic proton beams

Vincenzo Monaco[1,2], Omar Hammad Ali[3], Davide Bersani[4], Mohammed Abujami[1,2], Maurizio Boscardin[3,5], Nicolò Cartiglia[2], Gian Franco Dalla Betta[5,6], Emanuele Data[1,2], Marco Donetti[7], Marco Ferrero[2], Francesco Ficorella[3], Simona Giordanengo[2], Oscar Ariel Marti Villarreal[3], Felix Mas Milian[1,2,8], Mohammad-Reza Mohammadian-Behbahani[9], Diango Montalvan Olivares[1,2], Marco Pullia[7], Francesco Tommasino[5,6], Enrico Verroi[3], Anna Vignati[1,2], Roberto Cirio[1,2] and Roberto Sacchi[1,2]

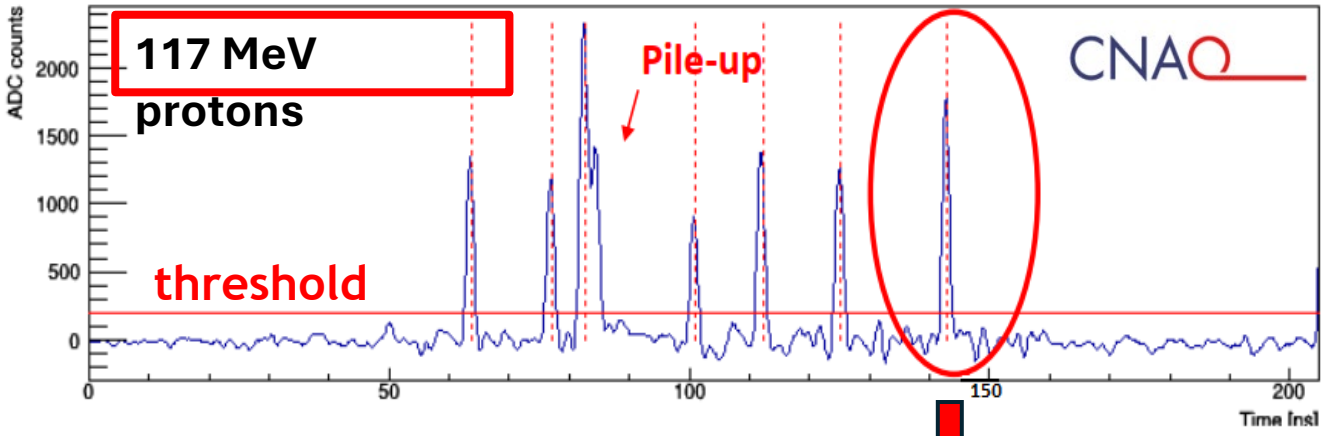

Strip sensors readout by digitizer

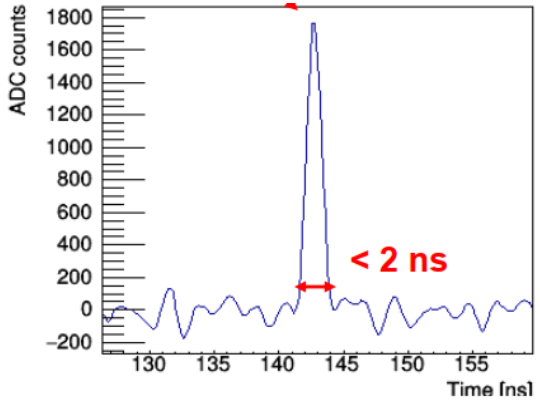

- Short peak duration
- Large Landau fluctuations
- Single particle discrimination
- Signal pile-up

Carbon ion signals and time resolution

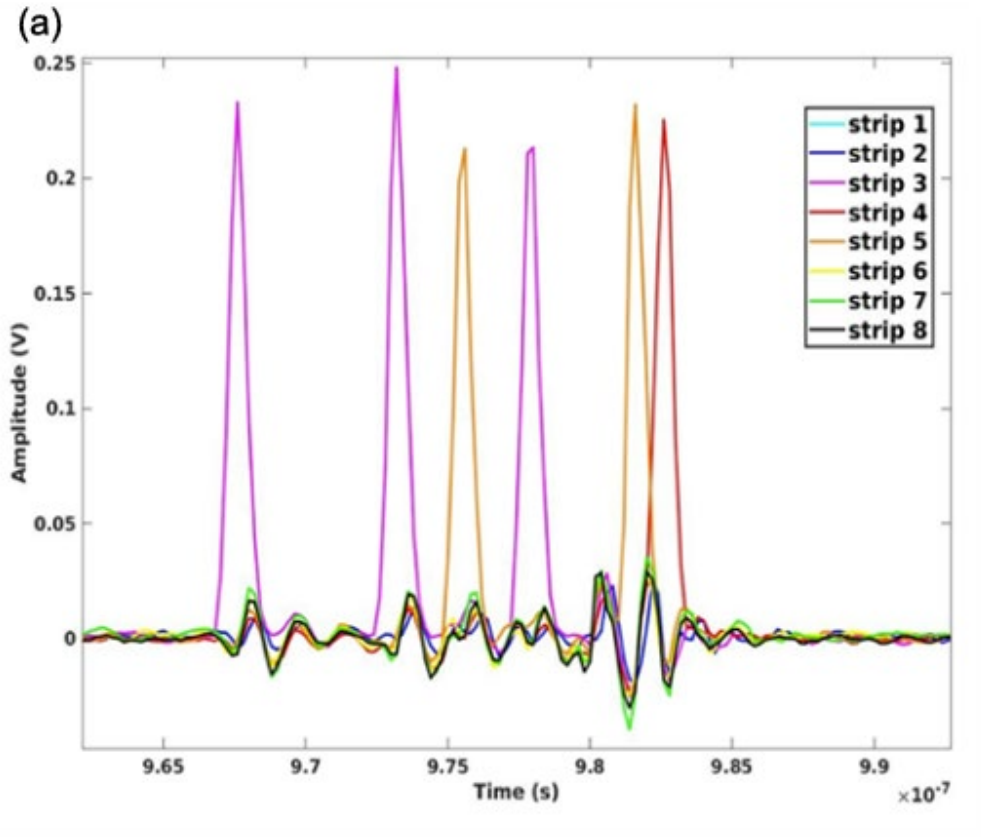

Physica Medica 2025

Thin segmented silicon detectors for single ion tracking in carbon ion beam therapy: Performance insights

D.M. Montalvan Olivares [a,b] · F. Mas Milian [b,c] · O.A. Marti Villarreal [d] · ... · V. Sola [a,b] · A. Vignati [a,b] · S. Giordanengo [b] ... Show more

10.1016/j.ejmp.2025.105048 External Link

Volume 136, 105048, August 2025 · *Open Access*

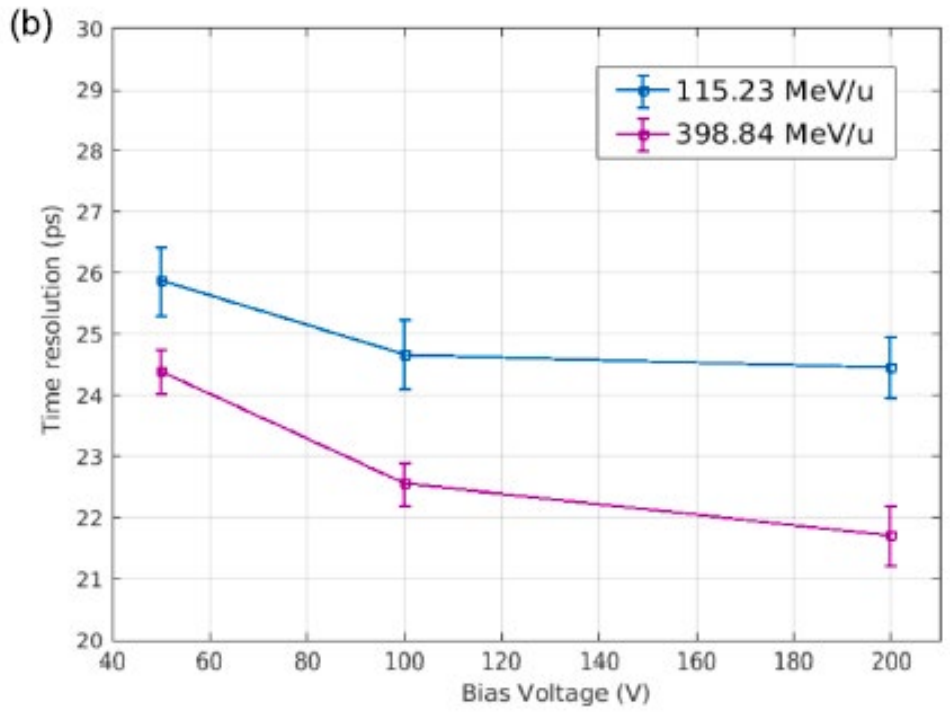

Prompt gamma detectors

- Cylindrical LaBr3(Ce) scintillating crystal (diameter = 3.81 cm, height = 3.81 cm)

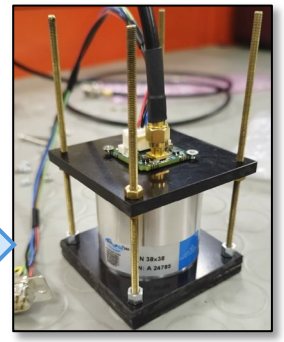

- 5x5 SiPM matrix, 24x24 mm^2 (FBK)
- custom board to sum up all SiPM signals

From FOOT experiment

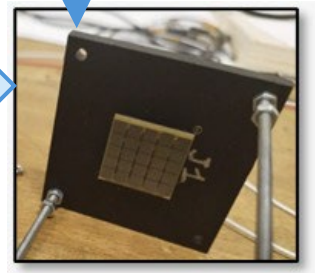

- Time resolution of about 200 ps

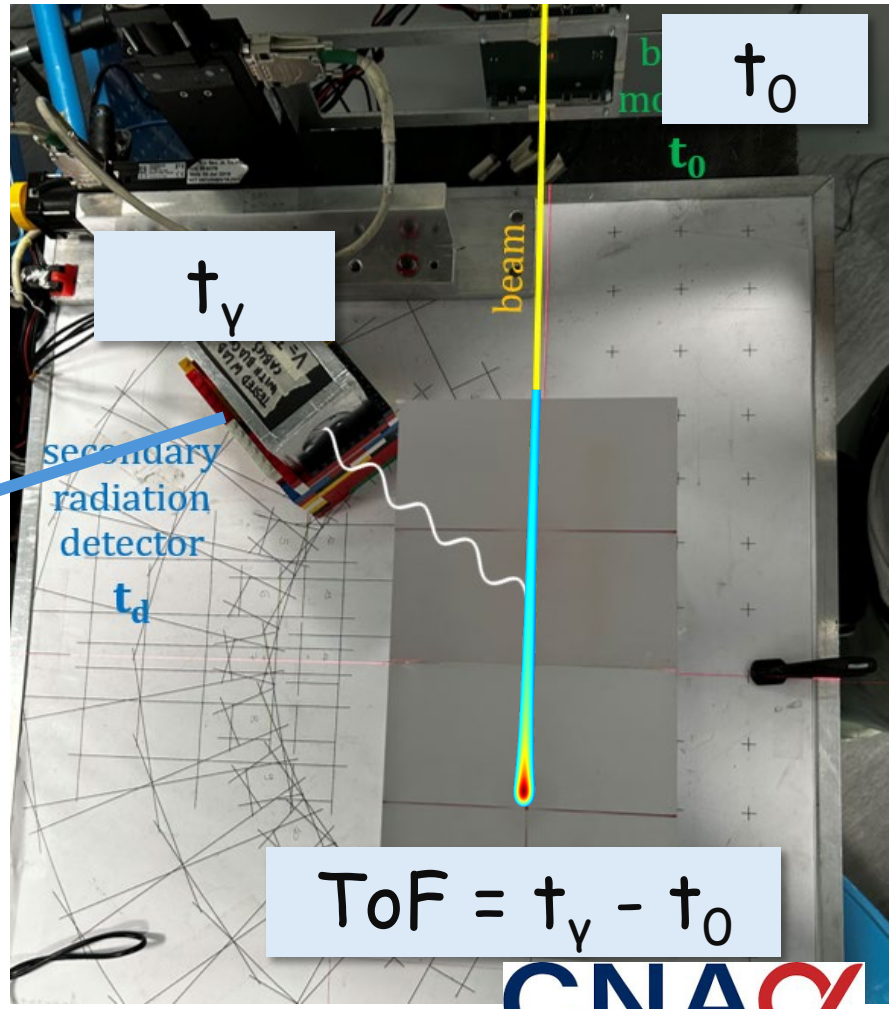

CNAO 23
Centro Nazionale di Adroterapia Oncologica

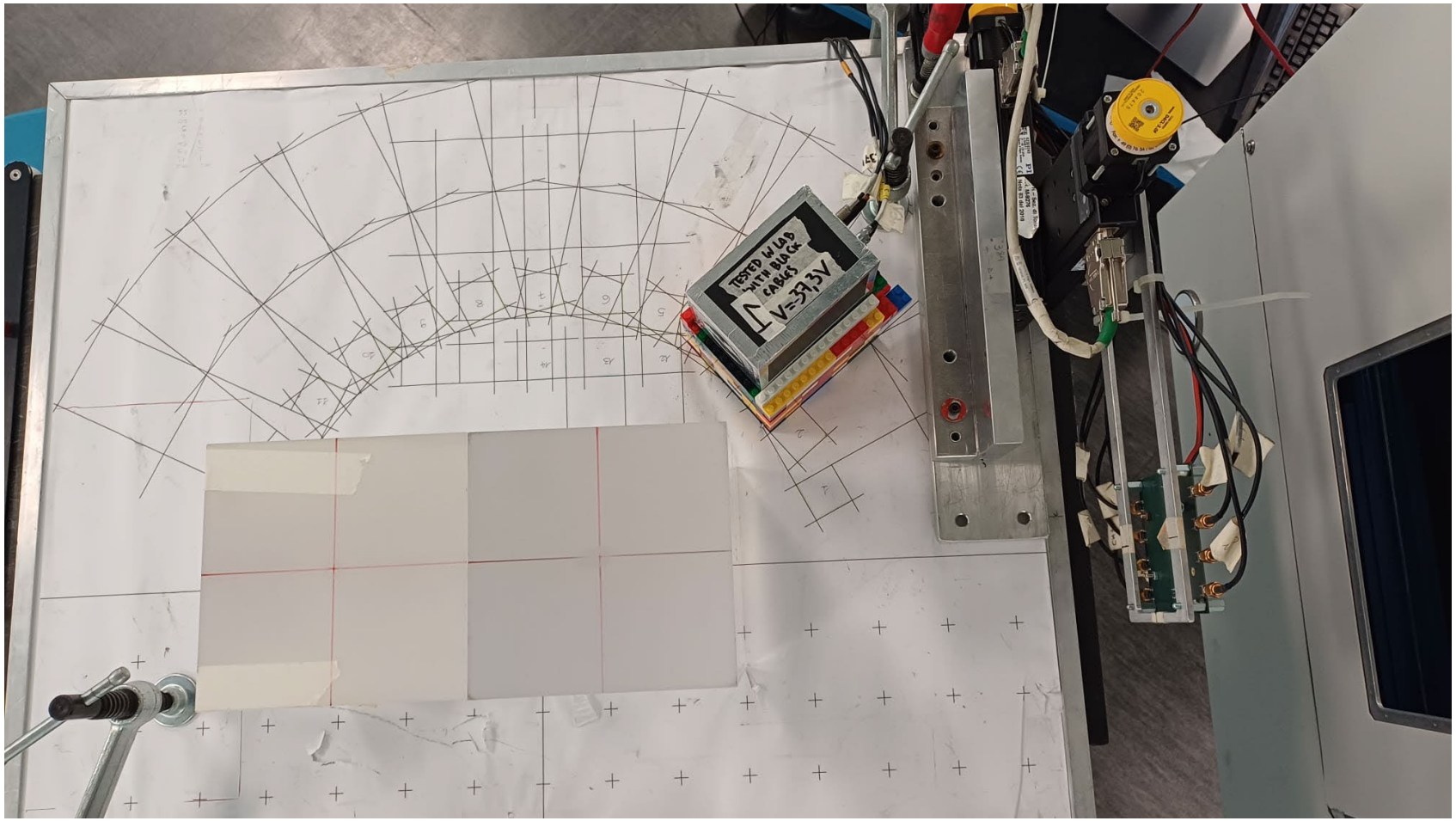
TESTED W LAB
WITH BLACK
CABLES
V=3.3V

PGT measurements with carbon ion at CNAO

Carbon ion beam:

- Carbon ion energy = 399 MeV/u
- Subclinical particle rate:
  - Average rate = 5 x 10^6 particles/s (10 % of clinical rate)
  - Instantaneous rate = 2 x 10^8 particles/s

Phantom configurations:

1. 30-cm long homogeneous PMMA phantom
2. PMMA phantom with an air gap of 2 cm (full phantom length L = 32 cm)
3. PMMA phantom with an air gap of 4 cm (L=34 cm)
4. PMMA phantom with a bone slab of 1 cm (L=31 cm).

PG detector positions

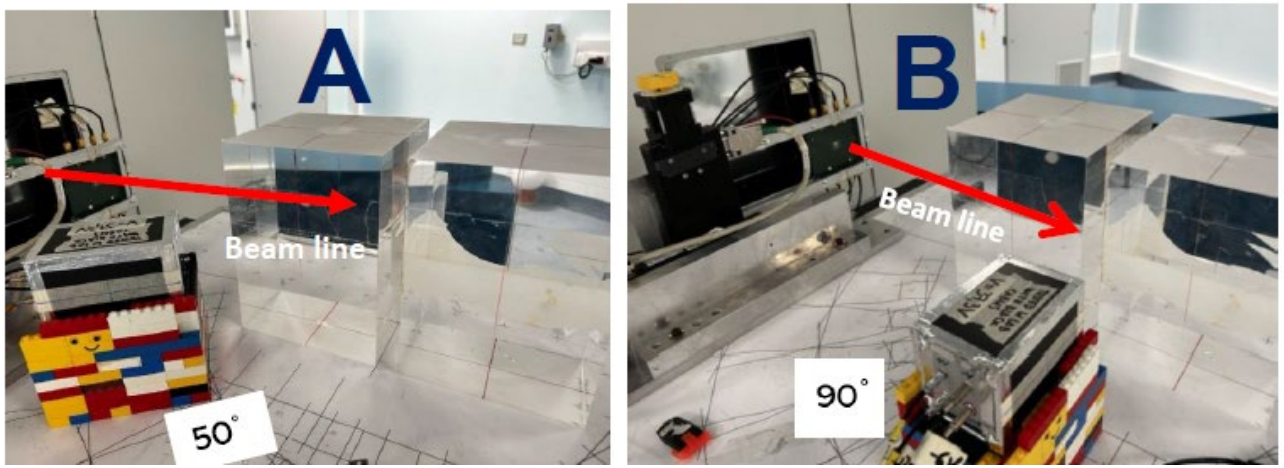

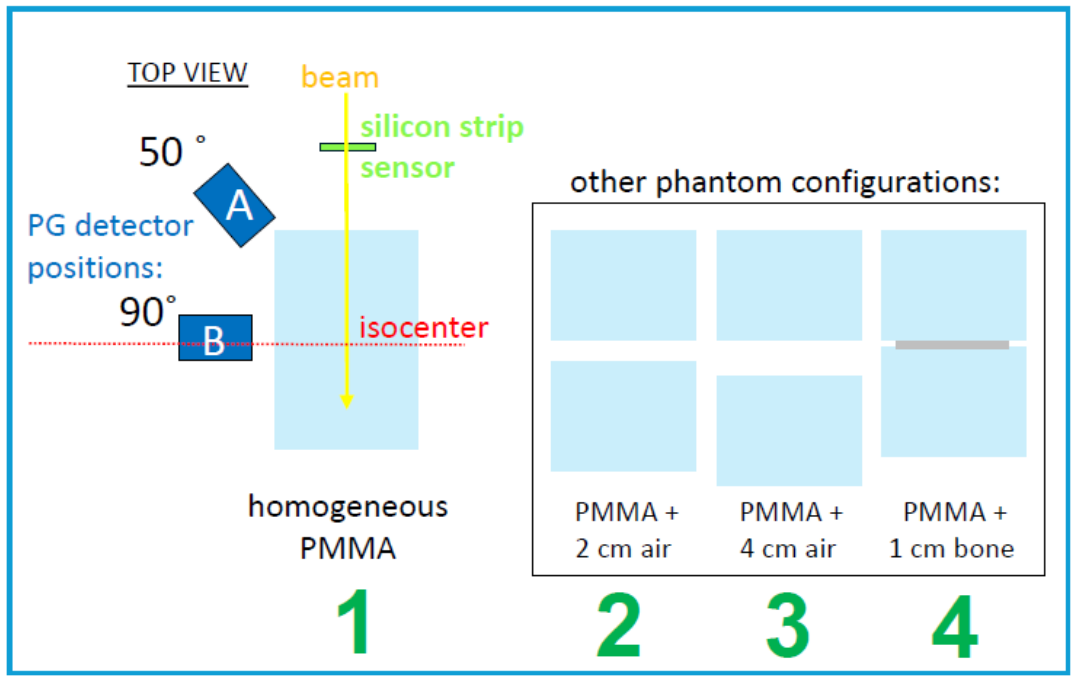

Waveform example (event)

DAQ system

CAEN digitizer 16-ch (DT5742)

- Signal read-out sampling freq 2,5 GHz
- Times at a constant fraction of the signal amplitude (CFD)

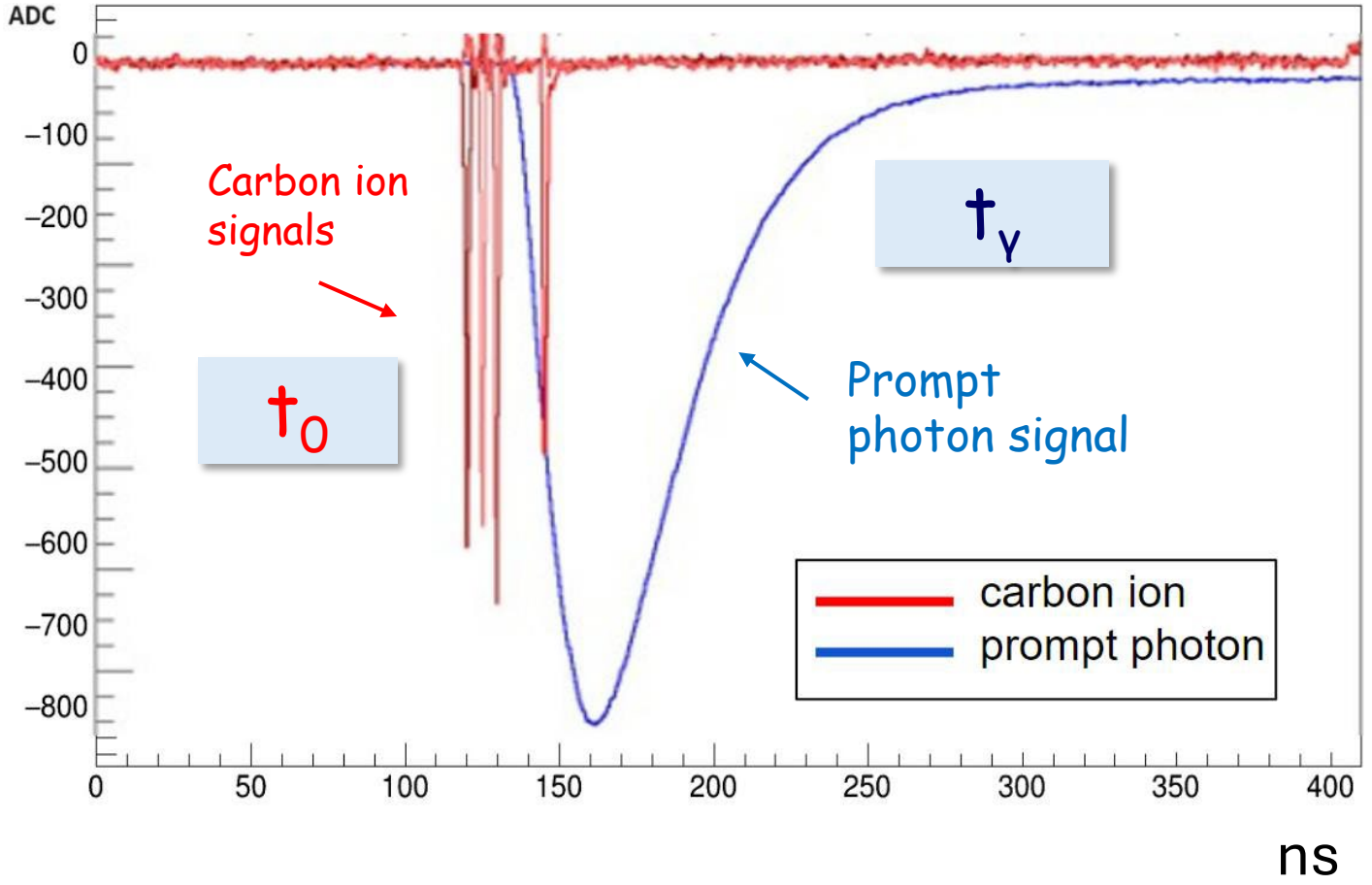

TOF distributions

- ToF distribution: difference between PG detector signal and all signals in the primary beam monitor

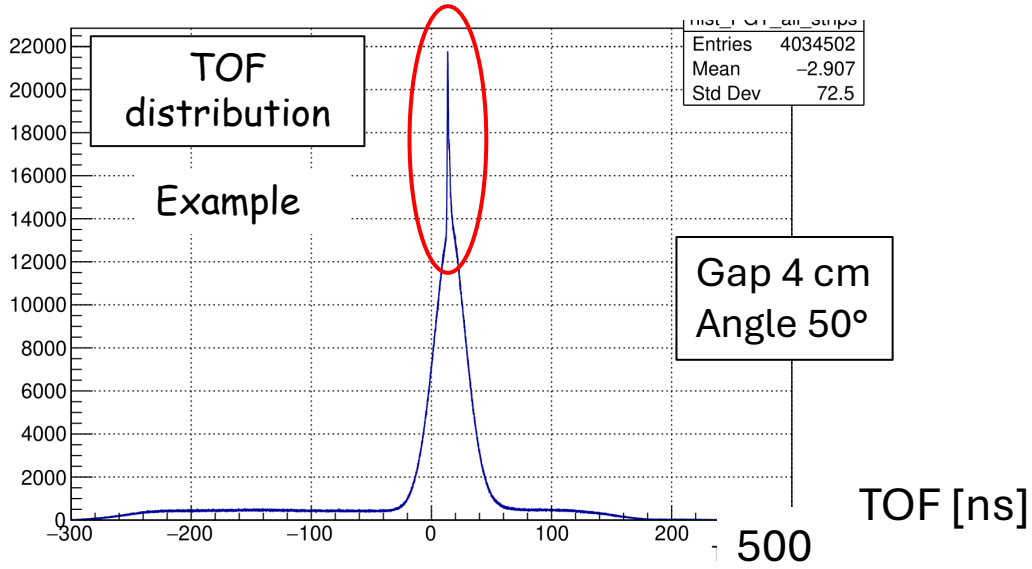

TOF distributions

- ToF distribution: difference between PG detector signal and all signals in the primary beam monitor
- **Combinatorial background** found with iterative peak detection algorithm then removed from TOF distribution
- **Distribution normalization** based on the time interval corresponding to the region where phantoms are equivalent (rising edge of the distribution)

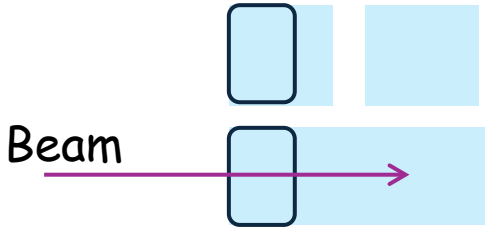

Normalization region

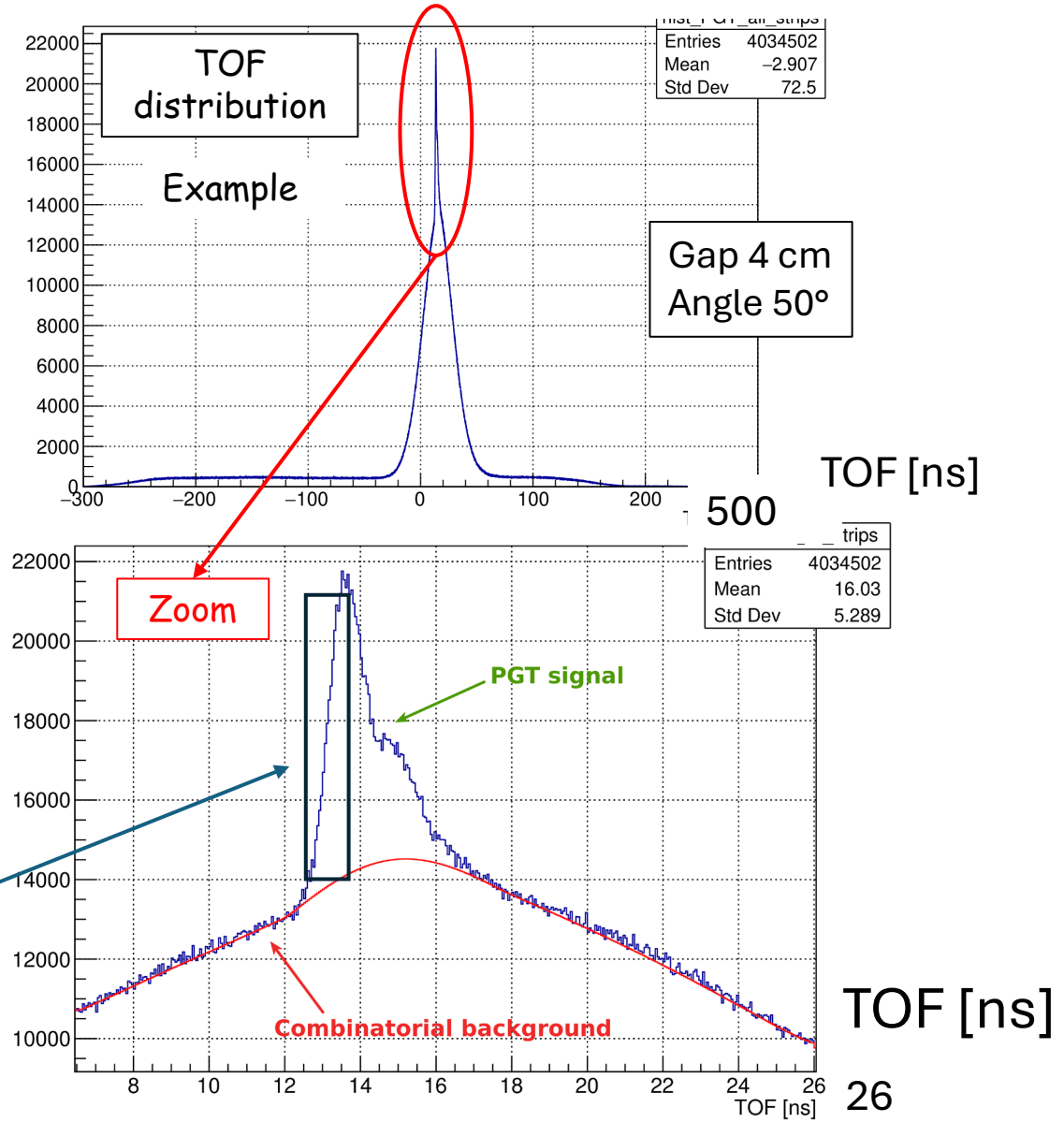

Statistical error of PGT distributions

Subset extraction: for each phantom geometry

-Select randomly 2000 subsets from the whole dataset

-Considering a certain number of events (200k and 400k).

PGT distribution:

For each subset the final PGT distribution was obtained following the described procedure.

Confidence interval calculation:

-Considering all the PGT distributions for each subset:

-Calculate 2.5% and 97.5% percentiles for each time bin
→ define the 95% confidence interval for each phantom geometry.

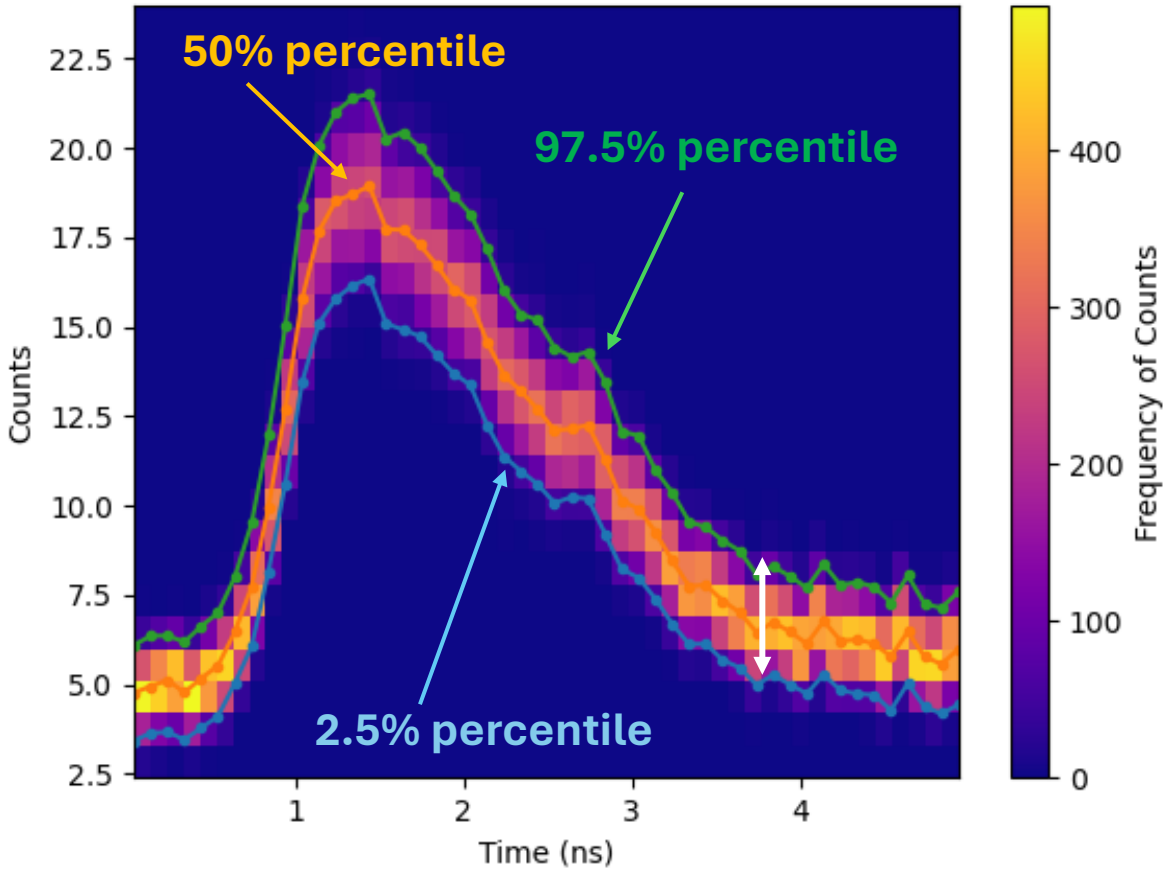

Results of measurements acquired with digitizer

- Error band corresponds to 95 % confidence interval
- The air gap results in the hole around 2 ns in the PGT distribution measured at 50 °

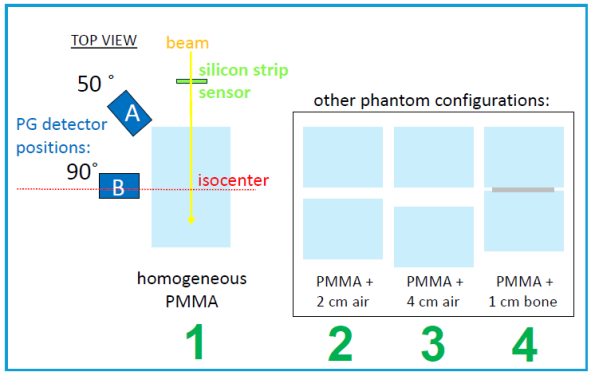

PG detector at 50°

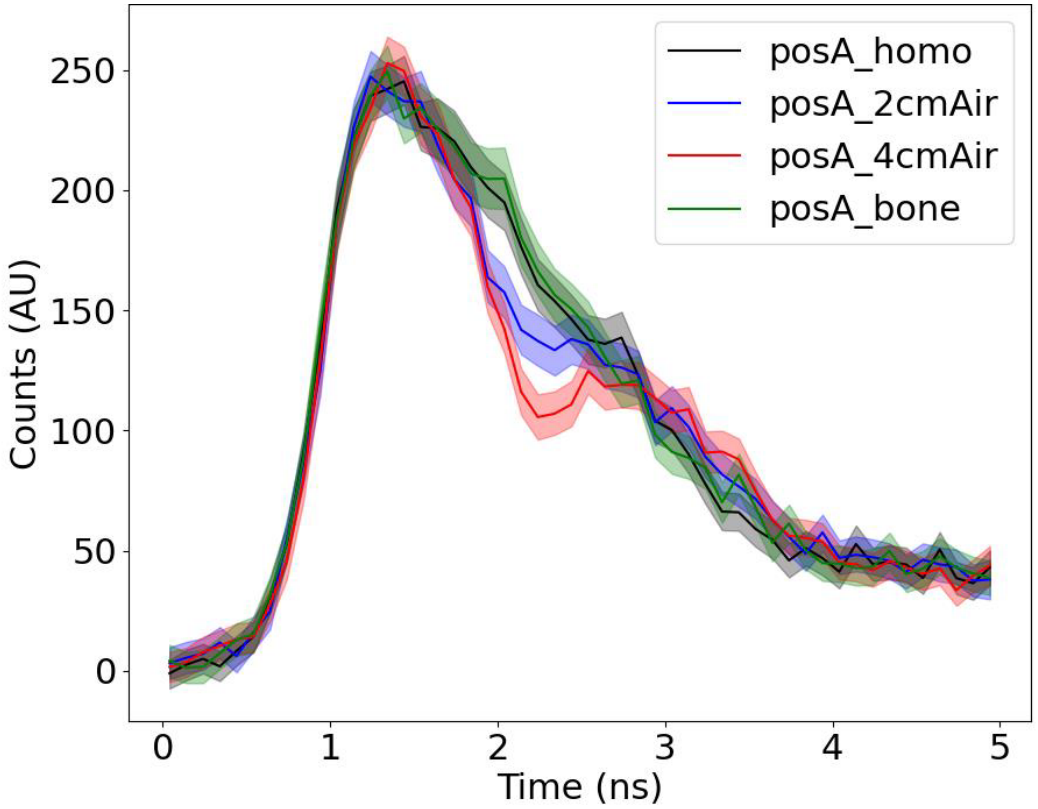

PG detector at 90°

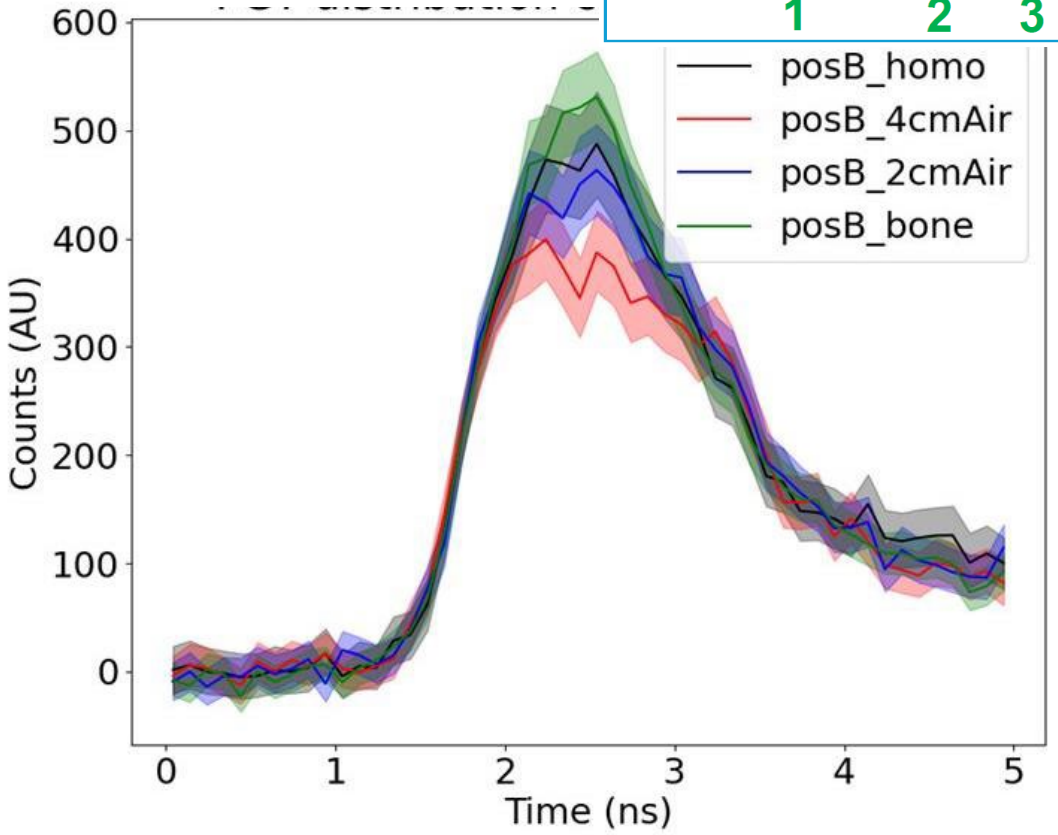

Compatibility between distributions PG detector at 50°

For each bin:

Compatibility (probability) = $\frac{\text{Number of subsets}_x \text{ within 95\%CI of subset}_{homo} \text{ distribution}}{\text{Total number of subsets}_X \ (=2000)}$

- Homogeneous PMMA phantom distribution considered as reference distribution
- For each bin, how many subsets from a different geometry (x) fall within the 95 % confidence interval of the reference?

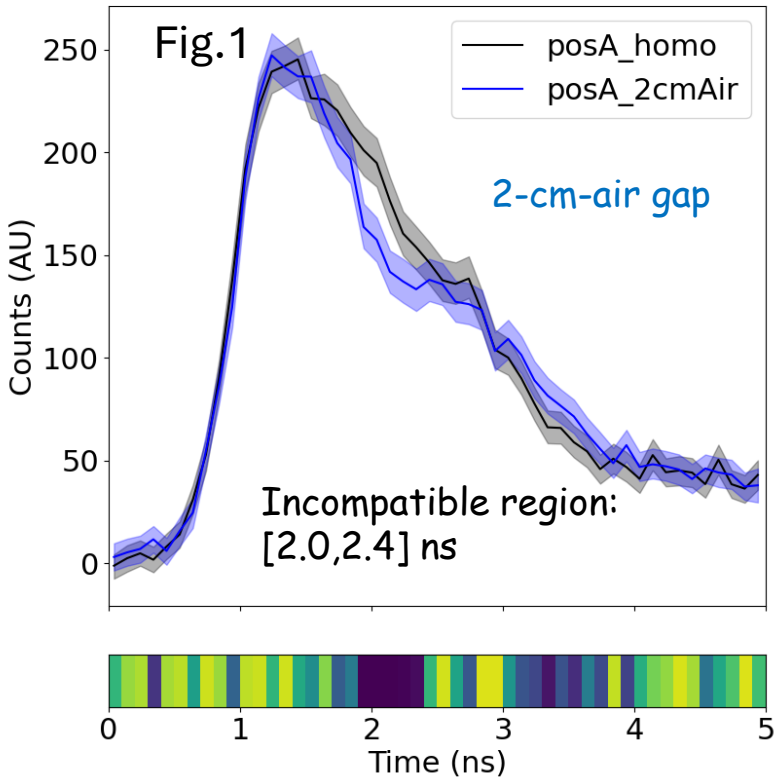

Degree of compatibility between distributions - PG detector at 50°

- Homogeneous PMMA phantom distribution considered as reference distribution
- For each bin, how many subsets from a different geometry (x) fall within the 95 % confidence interval of the reference?

For each bin:

Compatibility (probability) = $\frac{\text{Number of subsets}_x \text{ within 95\%CI of subset}_{homo} \text{ distribution}}{\text{Total number of subsets}_X \text{ (=2000)}}$

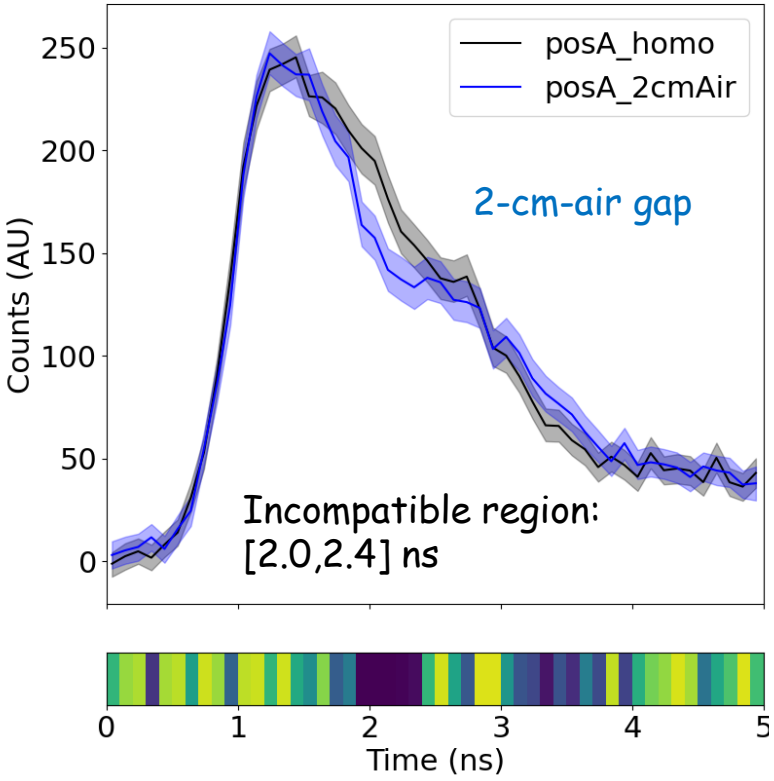

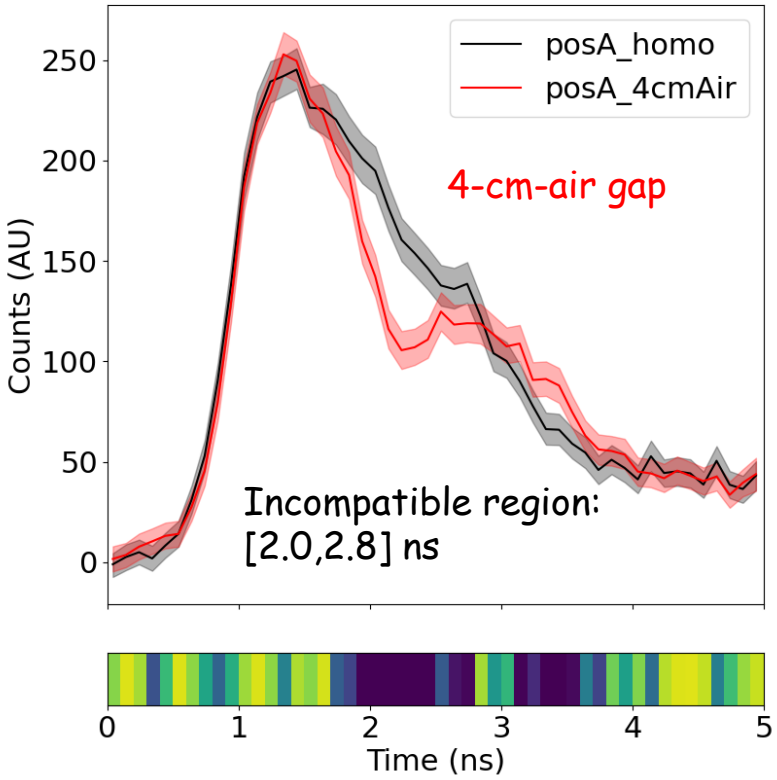

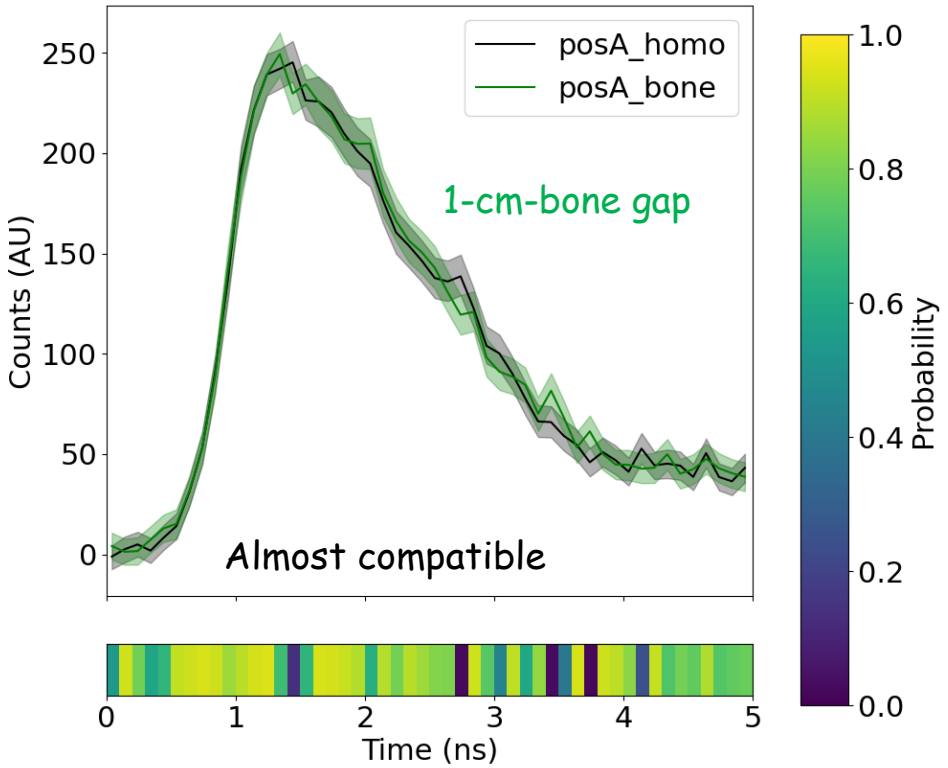

Degree of compatibility between distributions - PG detector at 90°

- Homogeneous PMMA phantom distribution considered as reference distribution
- For each bin, how many subsets from a different geometry (x) fall within the 95 % confidence interval of the reference?

For each bin:

Compatibility (probability) = Number of subsets$_x$ within 95%CI of subset$_{homo}$ distribution / Total number of subsets$_X$ (=2000)

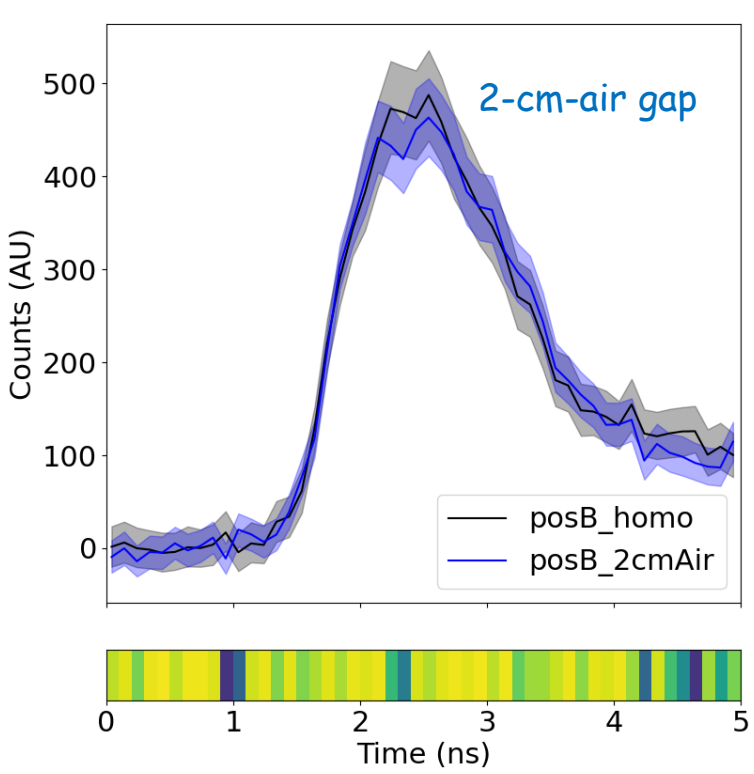

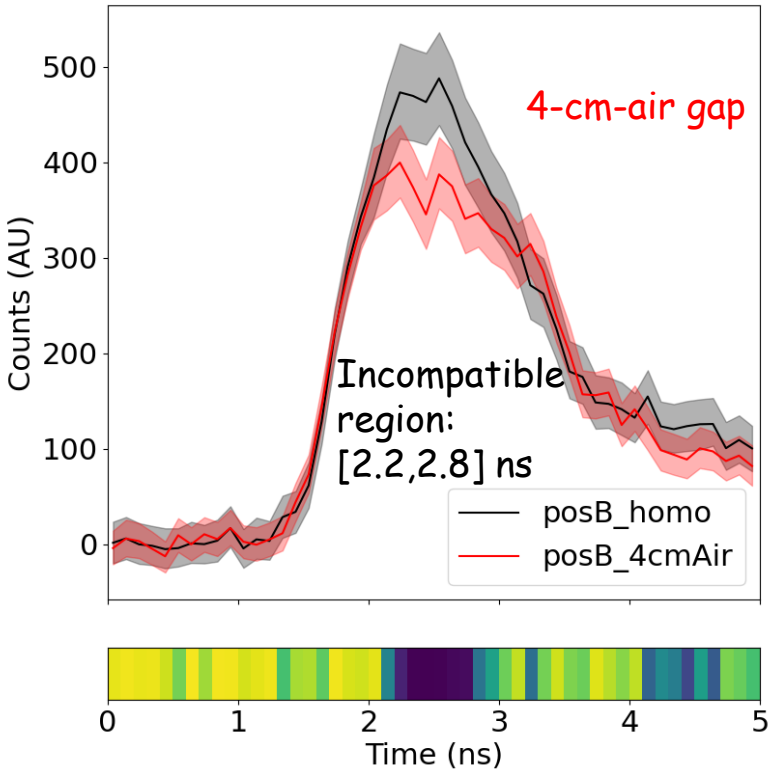

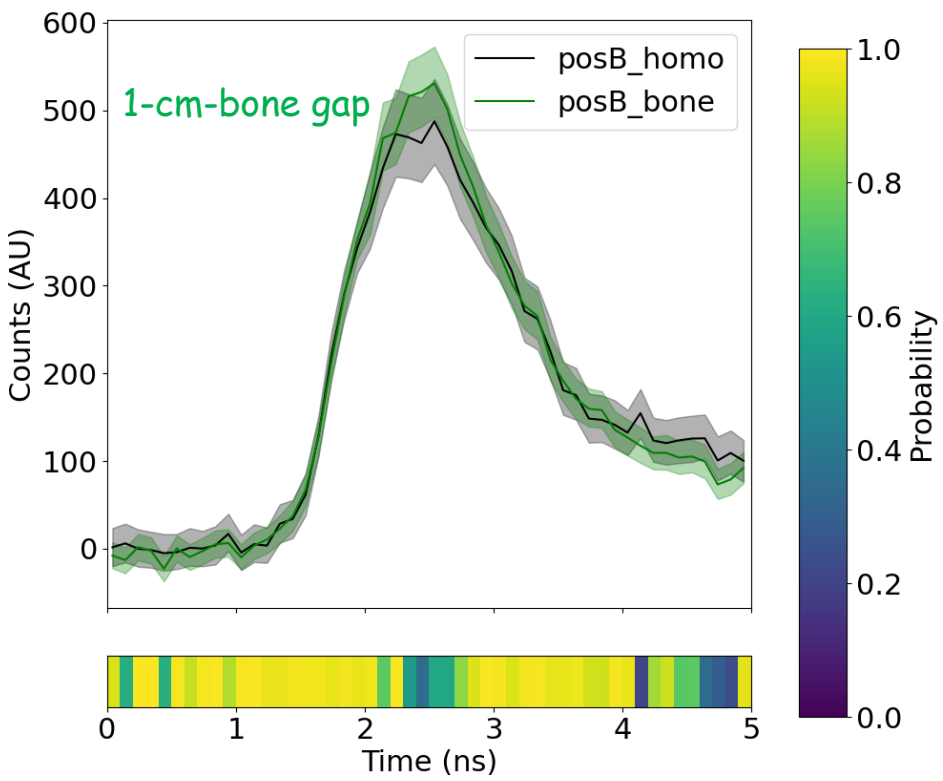

Experiment vs simulation – homogenous phantom

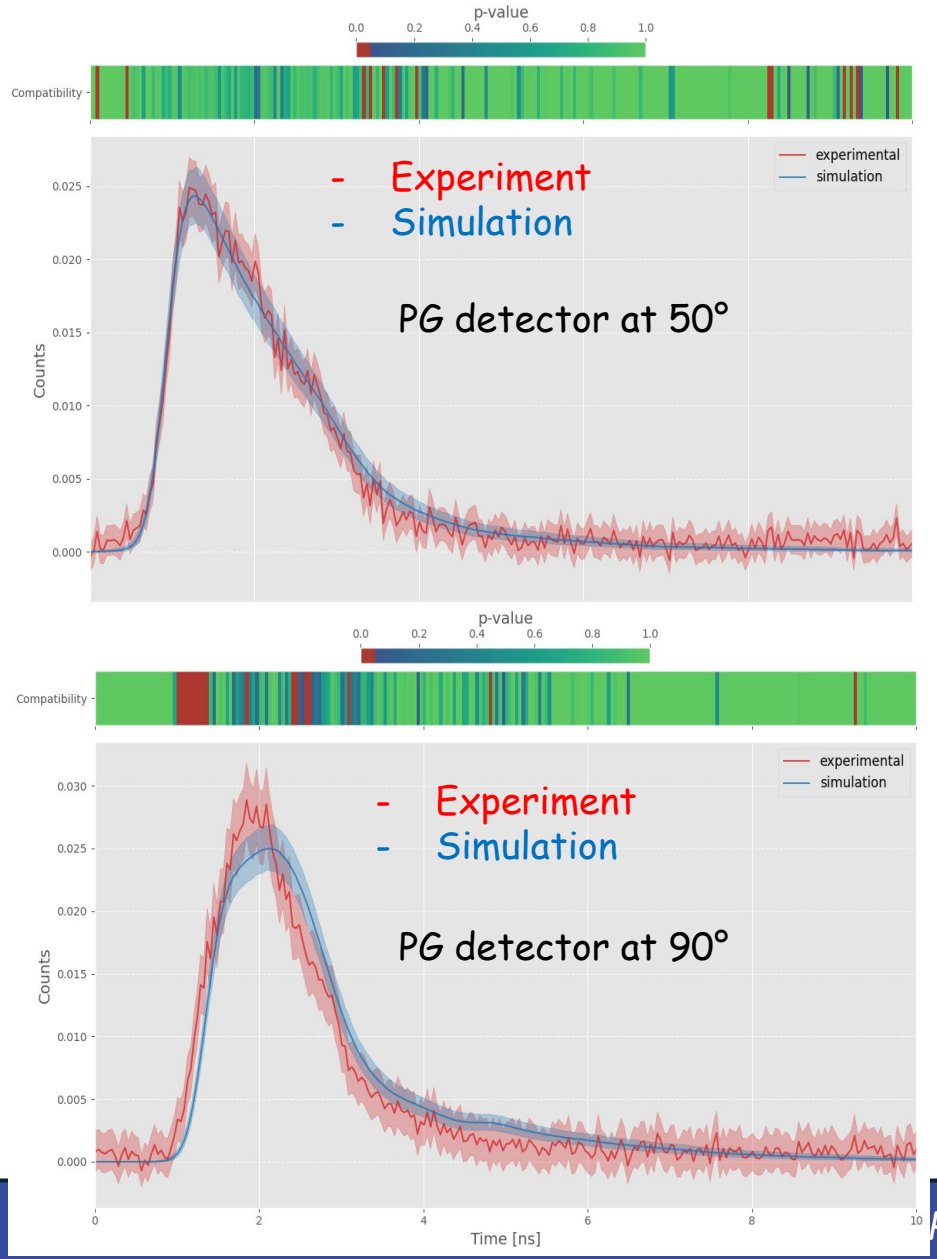

- Good agreement with simulations of PGT measurements performed with Fluka
- Different components of the PGT distributions can be retrieved from the simulation:
  - Photons, protons, neutrons, electrons

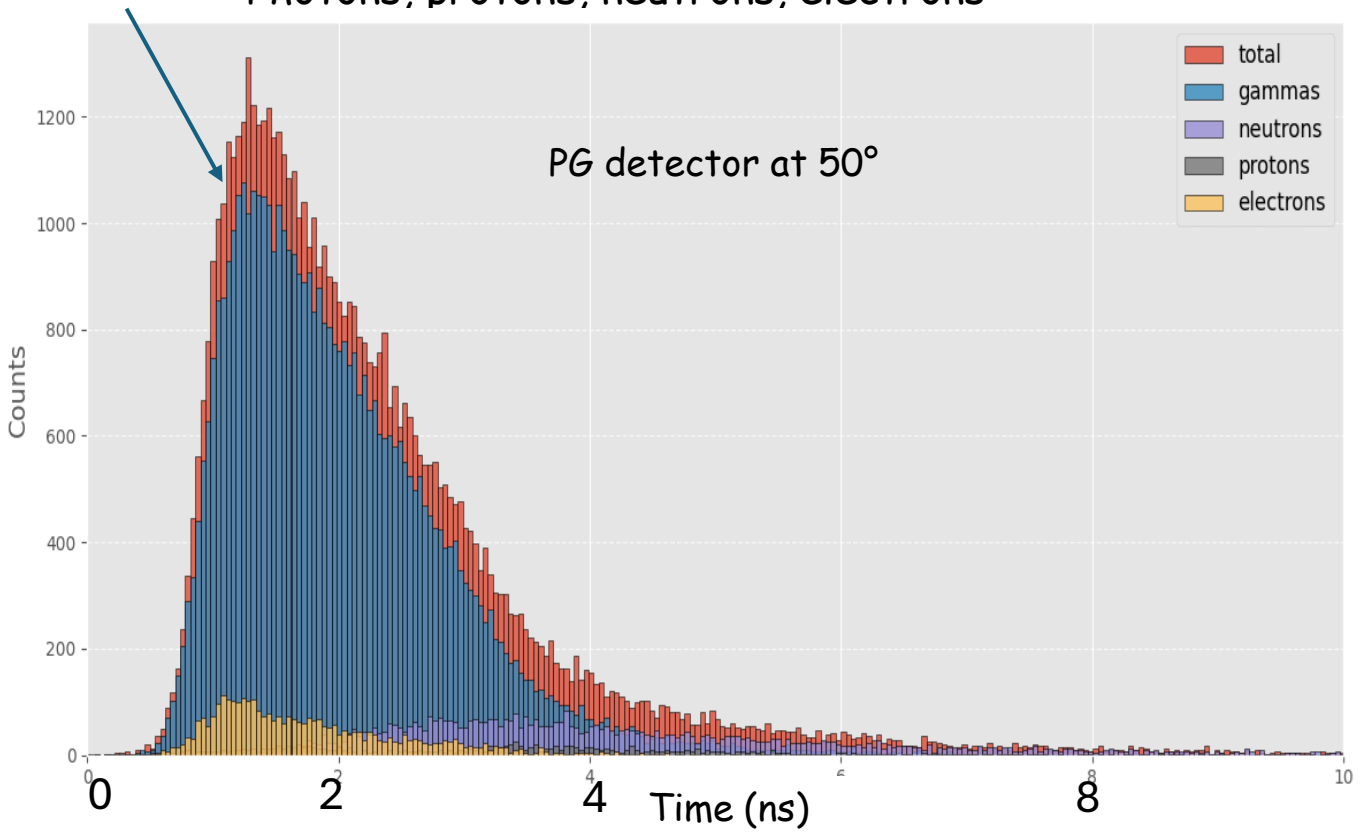

DAQ based on a Time to Digital Converter (TDC)

- Signals fed into 16-channel discrimination module (A5256)
- Time stamps measured with CAEN PicoTDC (DT5203)
- Time resolution of PG detector + PicoTDC measured in laboratory with Co60 = 300 ps
- Time walk correction for PG signals

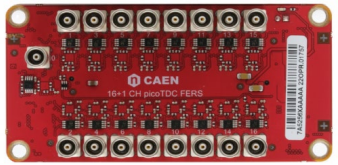

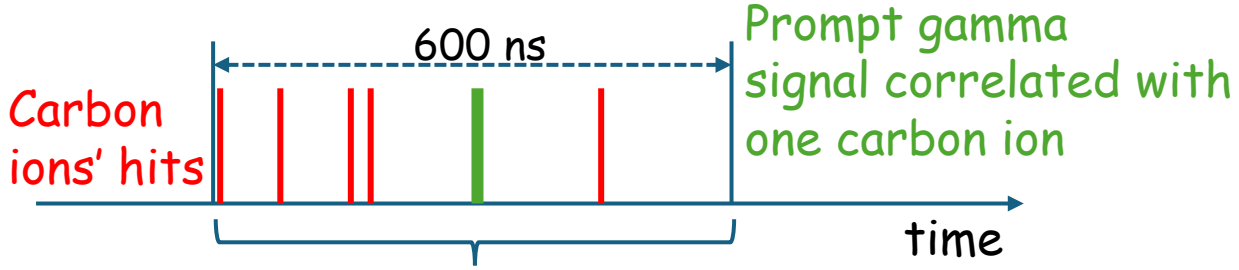

- Acquisition in trigger mode

- Time stamps in the window recorded
- $ToF^{(i)} = t_{gamma} - t^{(i)}_{ion}$

Preliminary results of measurements acquired with PicoTDC

- Distributions normalized to the first part of the distribution which is expected to be independent of the air gap
- The 4-cm-air gap results
  - hole around 2 ns in the PGT distribution measured at 50°

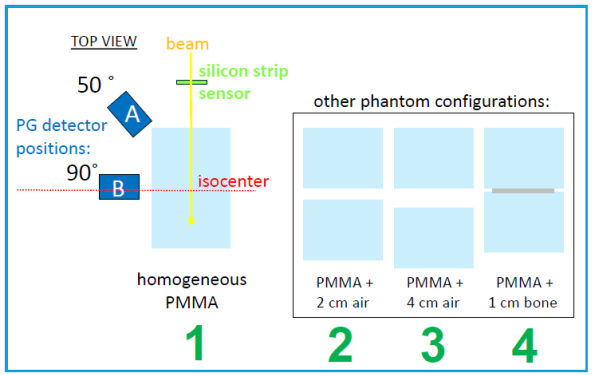

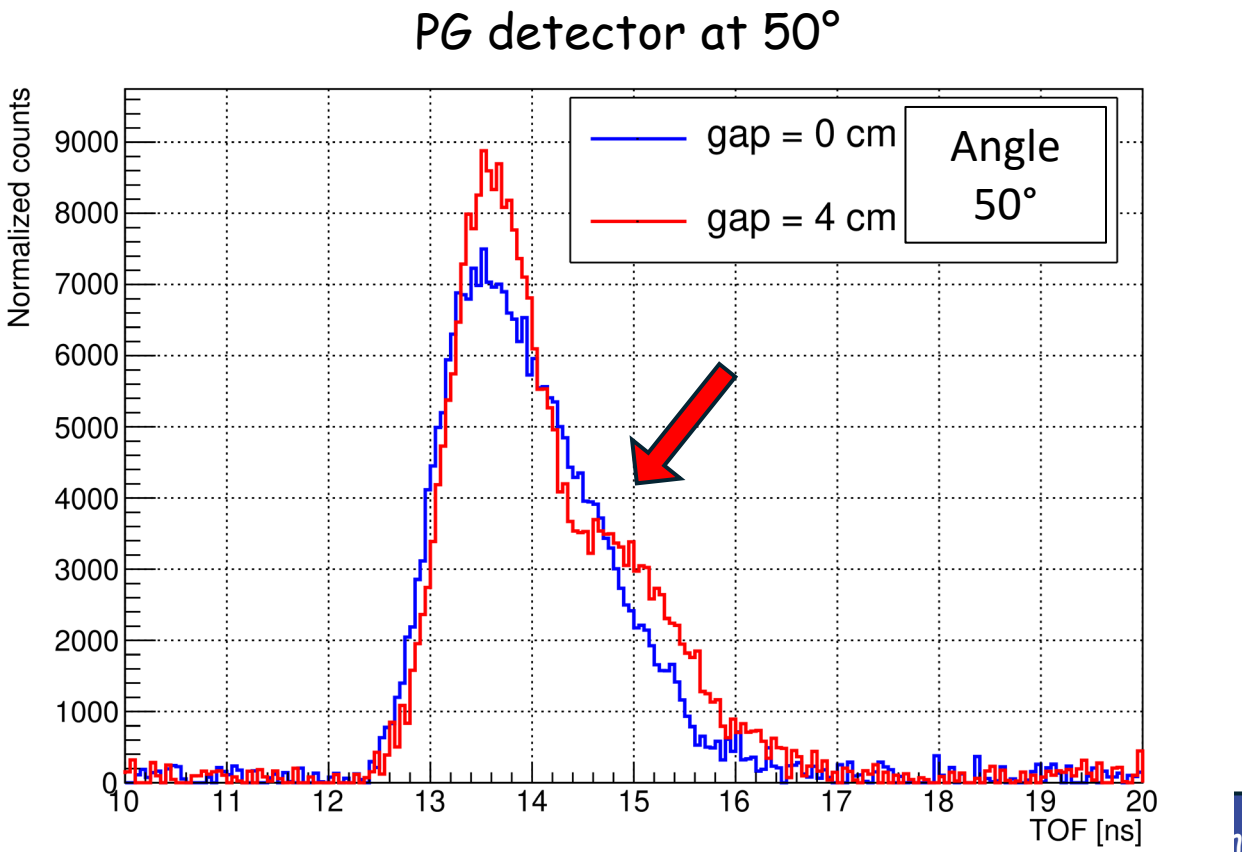

Preliminary results of measurements acquired with PicoTDC

- Distributions normalized to the first part of the distribution which is expected to be independent of the air gap
- The 4-cm-air gap results
  - hole around 2 ns in the PGT distribution measured at 50°
  - Broader distribution with PG detector at 90°

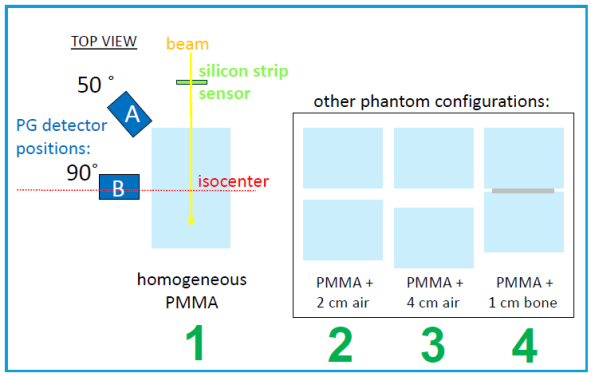

PG detector at 50°

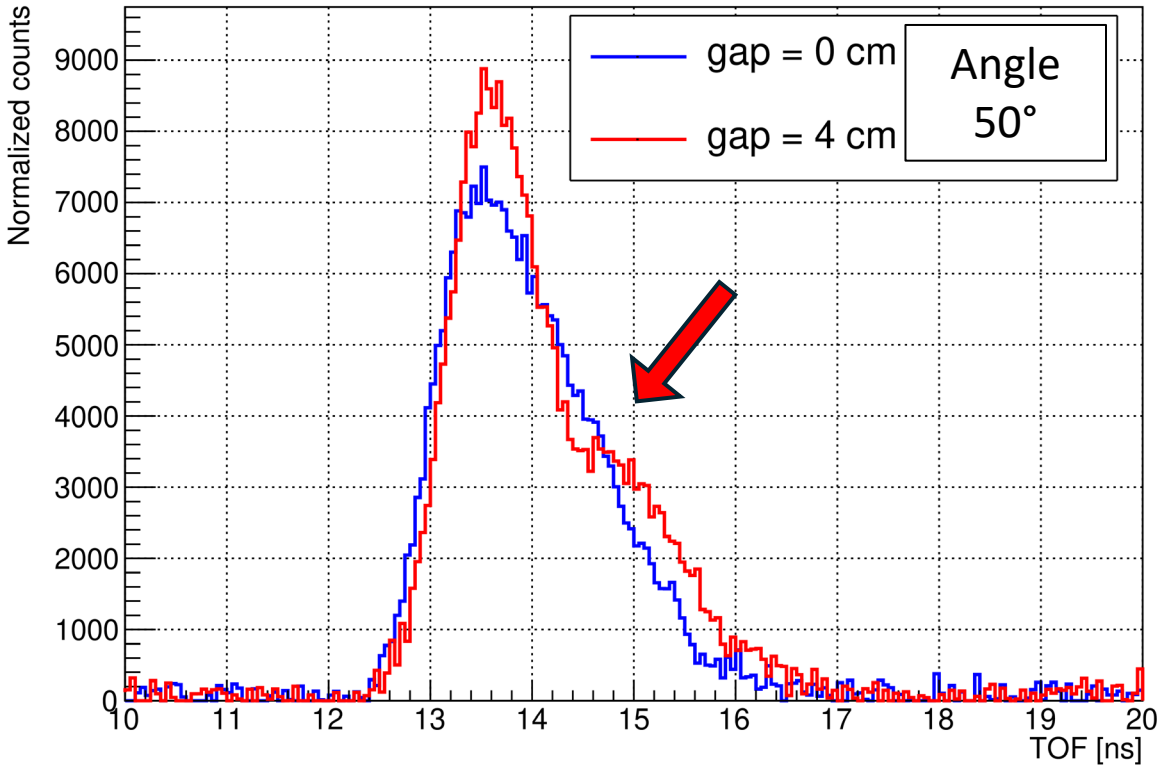

PG detector at 90°

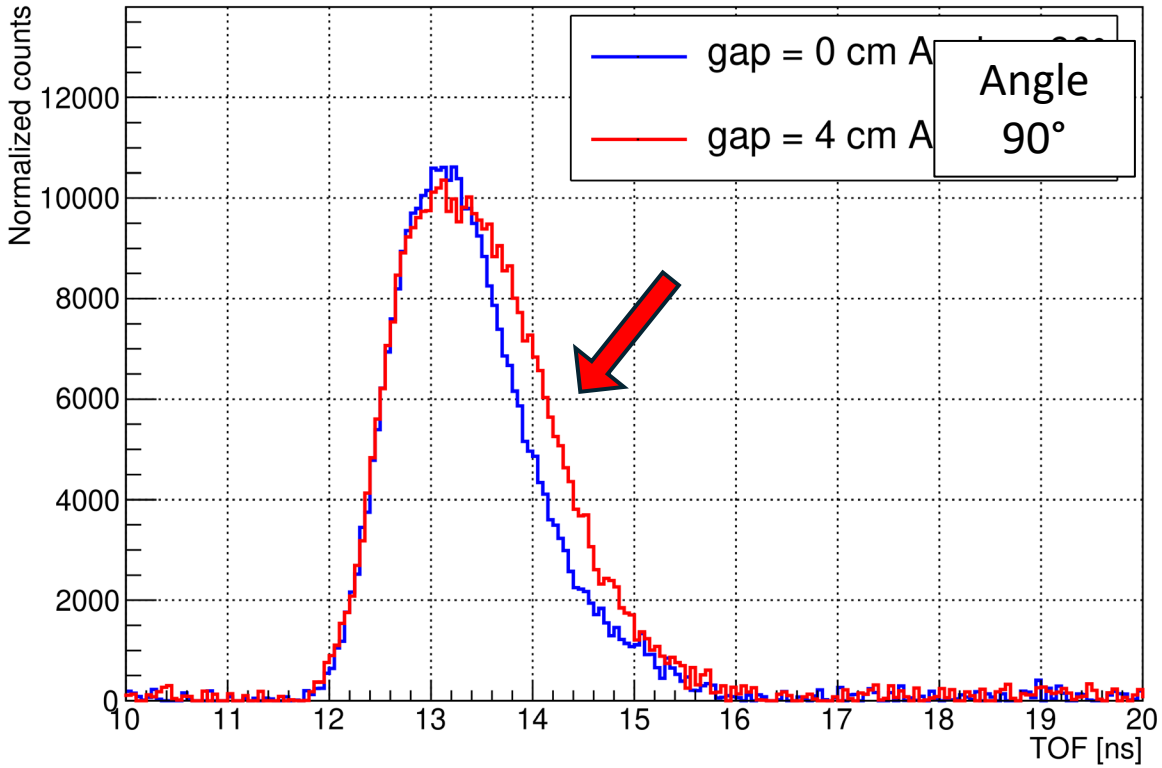

Summary

- Preliminary PGT system was developed and tested at CNAO with carbon ions
- Distributions with clinical carbon ions have been measured
- The system showed to be sensitive to a 2-cm-air cavity between two PMMA blocks
- System sensitivity to range variation depends on PG detector position

Future perspectives

- Optimized DAQ system with picoTDC to improve efficiency thanks to
  - faster readout
- 2.7x2.7 cm^2 detectors for primary particles
- More Scintillators and range reconstruction algorithms

Thank you for your attention

INFN

UNIVERSITÀ DI TORINO

CNAO
Centro Nazionale di Adroterapia Oncologica

FONDAZIONE BRUNO KESSLER

Backup slide

2.7×2.7 cm² particle counter (ESA ABACUS)

Silicon strip sensor
Strips width: 114 µm
Pitch: 180 µm
Active thickness: ~50 µm
Capacitance: ~7 pF

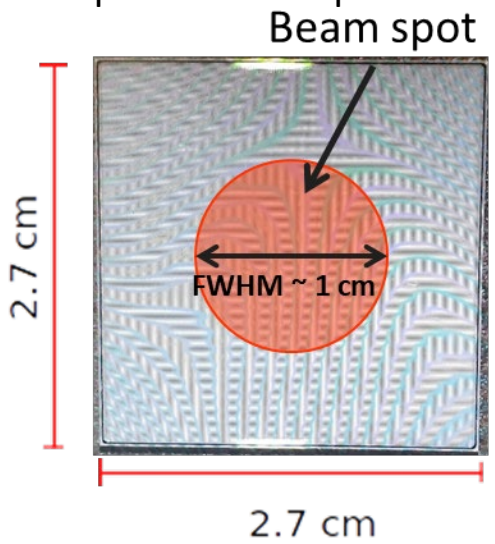

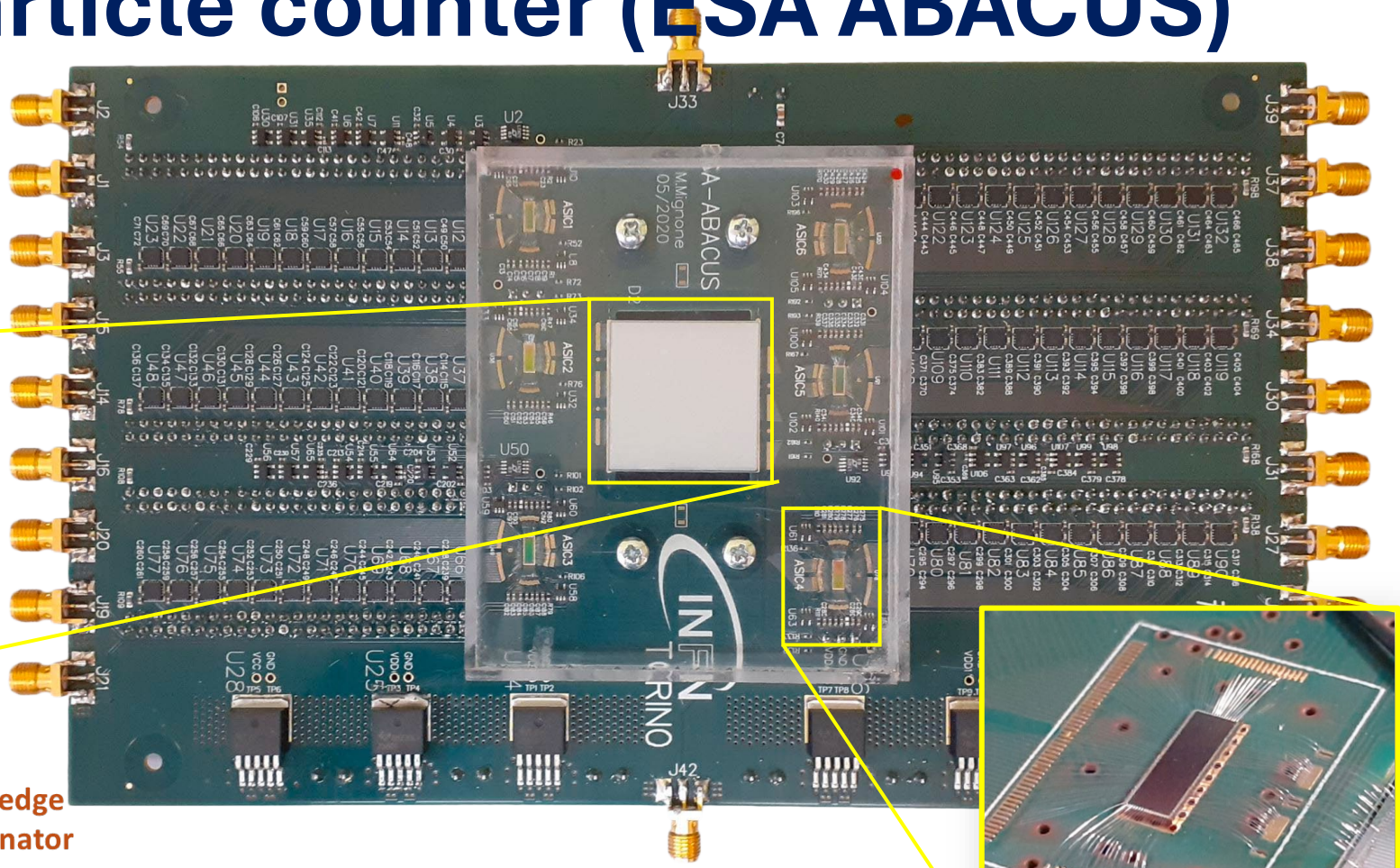

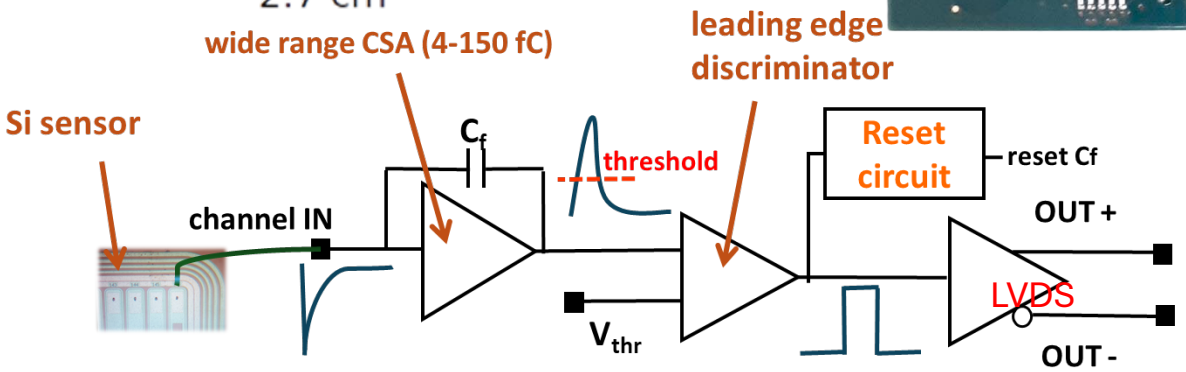

The ABACUS chip (x6)

- 110 nm CMOS technology, chip area = 2 × 5 mm², 24 channels, 144 in total. CSA dynamic range: 4 fC – 150 fC. Dead time : ~ 10 ns.